HUMAN NEURAL STEM CELL DIFFERENTIATION AND ELECTRICAL STIMULATION ON A NOVEL SINGLE WALLED CARBON NANOTUBE-POLYMER COMPOSITE

By

JEFFREY THOMAS TURNER

A thesis submitted to the

Graduate School-New Brunswick

Rutgers, The State University of New Jersey

and

The Graduate School of Biomedical Sciences

University of Medicine and Dentistry of New Jersey

In partial fulfillment of the requirements

For the degree of

Master of Science

Graduate Program in Biomedical Engineering

Written under the direction of

Dr. Prabhas V Moghe

And approved by

_____

_____

_____

New Brunswick, New Jersey

October 2013

ABSTRACT OF THE THESIS

HUMAN NEURAL STEM CELL DIFFERENTIATION AND ELECTRICAL STIMULATION ON A NOVEL SINGLE WALLED CARBON NANOTUBE-POLYMER COMPOSITE

By JEFFREY THOMAS TURNER

Thesis Director: Dr. Prabhas V Moghe

Increasing control of human neural stem cell (hNSC) differentiation is critical to development of cellular models for neurodegenerative diseases such as Parkinson's disease because current methods do not result in the required fully developed cells. In addition, existing cell culture and differentiation regimen are inefficient due to lengthy differentiation times and low yields of functional cells. The use of carbon nanotubes (CNTs), particularly in 3D geometries, offers a possible solution by improving the kinetics and efficiency of NSC differentiation. Electrical stimulation through conductive substrates, such as CNTs, can cause increased rates of NSC differentiation. In this work, a combination of a three dimensional, *in vivo* mimetic, single walled CNT substrate and electrical stimulation is used to investigate survival and differentiation behaviors of hNSCs derived from induced pluripotent stem cells (iPSCs). First, fibrous poly(lactic-co-glycolic acid) (PLGA) substrates, with an average fiber diameter of 1.11µm, are manufactured via electrospinning onto a flat plate collector. A novel vacuum driven impregnation technique forces an aqueous dispersion of CNTs to coat the PLGA fibers while maintaining the microscale features of the fibers' architecture. The CNTs provide increased electrical conductivity, >0.1 S/m up to 25 S/m, and nanosurface roughness, which can increase neurite interfacial interactions, resulting in improved differentiation of NSCs to neurons. Immunocytochemistry of hNSC differentiated on these surfaces reveal an 18% rise in the number of cells staining positive for neurofilament M (NFM), a marker of maturing neurons, on CNT versus control PLGA substrate after 14 days of differentiation. When a 10 minute, 30µA

direct current stimulation is applied on the 3rd day of differentiation, there is a further 4% improvement in the number of cells staining positive for NFM on the 14th day of differentiation. Calcium imaging indicates that on day 14, 0.3% of cells on PLGA scaffolds compared to 5.9% of cells on the CNT composite substrate had an electrical event in response to electrical stimulation. These results strongly support the use of electrically conductive CNT substrates for neural differentiation and suggest electrical cues could be more systematically investigated for directing the differentiation process to sub-type specific and functional human neuronal systems.

Acknowledgements

I would like to thank Dr. Prabhas Moghe, my committee, and the entire Moghe Lab group. In particular Aaron Carlson, Neal Bennett, and Jocie Cherry. Neal was very helpful throughout my time at Rutgers, always willing to lend a helping hand, and since we came in at nearly the same time we learned almost everything together. I wish you luck on the road to your PhD. Aaron Carlson was instrumental in my development as a researcher and taught me everything I know about laboratory techniques. He was crucial to me learning to plan and analyze experiments as well as being a constant source of mentoring and an example of a stellar work ethic. My collaborators John and Greg in the lab of Dr. Neimark also deserve recognition for their willingness to discuss new ideas and provide me with more scaffolds whenever I needed them.

Finally I would like to thank my fiancée Joanna and my family, both of whom supported me through disappointments and triumphs. I am looking forward to spending more time with them as my time at Rutgers comes to a close.

Table of Contents

List of Illustrations/Tables

Chapter 1 – Introduction

hiPSC Derivation and Properties

Obtaining primary human neurons is challenging because biopsies of a living human brain are overly invasive, as primary human neurons deteriorate very quickly after the host's death, and the cells lose their functional phenotype once in culture [1]. The development of embryonic stem cells and induced pluripotent stem cells has made the derivation of human neural cultures possible, and a large effort is currently going into studying these cells. In 2007, the first human derivation of induced pluripotent stem cells (hiPSCs) used four separate integrating retroviruses to induce expression of the transcription factors: Oct4, Sox2, Klf4, and c-Myc [2]. These hiPSCs behave in the same way as human embryonic stem cells (hESCs) but were derived from fibroblasts instead of a human embryo. This difference is vital for several reasons. First, without the need for a destruction of a human embryo the ethical concerns of hESCs are alleviated. Second, the hiPSCs can be derived from an adult human patient with a medical history. Any genetically based diseases that person exhibits or will exhibit can be modeled when the appropriate cell type or types is derived from the hiPSCs made from their skin samples [3]. For example, dopamine neurons relevant to Parkinson's disease have been successfully derived from hESC using a growth factor based approach [4]. This concept of recapitulating disease phenotypes using hiPSCs derived from patients in this way has now been proven for a number of genetically inherited disorders. In a recent review by Bellin et al., the authors detail the advances in disease modeling in the fields of cardiovascular and neurology due to hiPSCs and find that 6 cardio-vascular, 12 neurological, and 6 mixed system disorders which have been partially or fully recapitulated *in vitro* using hiPSC derived cells. Human *in vitro* models for those diseases were not previously possible and so this advance could be significant in curing or

alleviating the symptoms of the those diseases [3]. In one example disease severity is claimed to be successfully modeled using appropriate patient samples [3]. The implementation of the pharmacological treatments are also shown to be effective at reducing disease systems, partially validating the system [5].

However, hiPSCs can develop problems due to the integrating nature of the original retroviruses, which operated by inserting copies of genes of interest into a host cell's genome. This insertion could result in the disruption of normal cellular function, which complicates model system producing these cells [6]. In some cases the aberrant functionality could be undetected until the lineage specificity is activated and then invalidate a large amount of time spent developing and testing a cell line. A simpler and more robust alternative would involve using a non-integrating or excisable system for ectopic gene expression. Examples include non-viral episomal vectors based on a derivative of the Epstein-Barr virus which transfects cells without the need for viral packaging. One group's plasmid was designed to express Oct4, Sox2, Nanog, Lin28, c-Myc, Klf4, and SV40LT combinations and resulted in the successful derivation of hiPSCs from human fetal foreskin [7]. Since the episomal vectors are deficient in replication without drug selection the resulting hiPSCs are quickly and easily cleared of plasmids. Although this method was published in 2009 as an improvement upon the original retrovirus derivation methods for hiPSCs, 76% of the literature on disease modeling still uses the original method and only 4% of the publications as of November 2012 use episomal vectors [3].

Conversion of hiPSCs to Neurons

Current differentiation techniques of human pluripotent stem cells (hPSCs) to neural cells can be divided into two categories: viral reprogramming methods and non-viral differentiation methods (**Figure 1-1**). Reprogramming methods offer the ability to derive neural cells very quickly from either a stem cell or somatic cell source [8]. The reprogramming approach has been shown

to result in functional neurons which appear to have the phenotype of several important brain regions including dopaminergic neurons and motor neurons [9, 10]. However, this approach generally results in very low reprogramming efficiencies demonstrated in 2010 [11] in mice and in 2011 in humans by the same group [8]. These cells may also be hampered from *in vivo* use because of viral integration into the cell's genome. Non-viral methods primarily rely on growth factors and substrate cues to go from hPSCs to a final neural phenotype, typically transitioning through a human neural stem cell (hNSC) phenotype. This thesis focuses on engineering the behaviors of NSCs in vitro. In fact, fetal hNSCs are already in clinical use for the treatment of amyloid lateral sclerosis with good safety indexes in phase I data [12]. However, the allogeneic nature of the treatment necessitated immunosuppressing drugs which would not be necessary with hiPSC derived hNSCs.

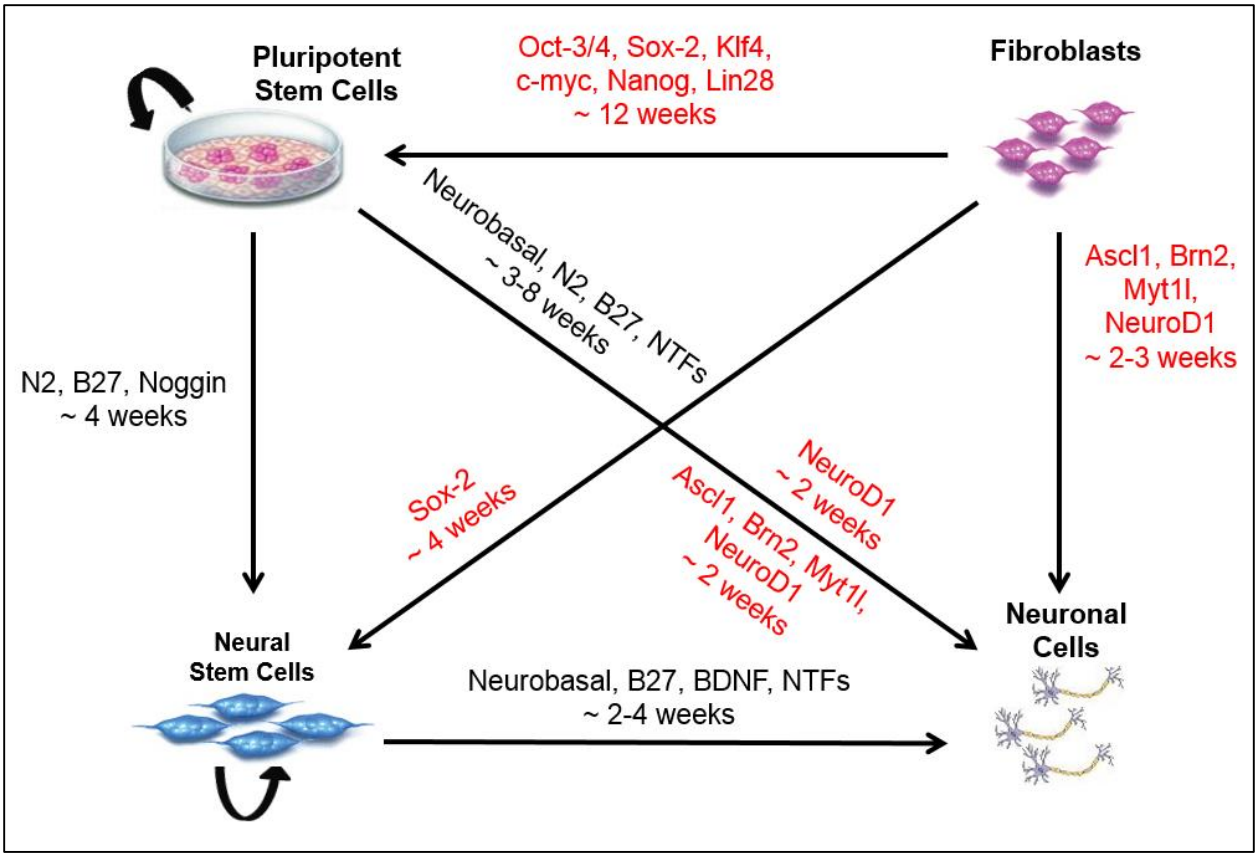

Figure 1-1: Methods for *In Vitro* Human Neuron Generation
The paths for generation of human neurons from a fibroblast source are shown. Methods written in red refer to reprogramming based modalities and black text refers to non-reprogramming methods. The approximate length of time for each step is shown underneath the primary media components or reprogramming factors required for each procedure. This figure was reproduced from the PhD Dissertation of Aaron Carlson [13].

There are numerous methods in the literature for deriving hNSCs from hPSCs such as hiPSCs. Several of these methods derived their mechanisms from the *in vivo* pathways during fetal and adult neurogenesis [14, 15]. Many methods rely on embryoid body formation, a co-culture with stromal cells, or the "default" differentiation pathway [15]. The embryoid body method relies upon the formation of ectoderm, mesoderm, and endoderm layer formation spontaneously within the embryoid body. The investigator then uses a media based selection method which yields neuronal cells with limited purity [15]. The co-culture method uses bone stromal cells to induce differentiation of sparsely plated hPSCs. Multipotent hNSCs result from this method, but the unknown factors delivered by the stromal cells make the cells ineligible for use in human

therapies [15]. The default differentiation pathway method is based on work which showed that in the absence of other factors *Xenopus* gastrula stage cells preferred to differentiate down the neural pathway, but that hypothesis has since been proven as overly simplistic [16]. Nevertheless, there is a translation for human use which operates by depriving PSCs of cell to cell contact and is very inefficient, making it unreliable for consistent use [15].

Methods for directed differentiation of adherent hPSCs to hNSCs via defined factors was an important step in the process of understanding neurogenesis and in the ability to generate neurons from hPSCs. One of the most widely cited methods was published in 2009 by Chambers et al [17]. Their method uses the growth factor Noggin and small molecule SB431542 to inhibit the SMAD pathway to induce neurogenesis. A large number of hNSCs can be produced using this method which are stable for 20 passages or more. A major advantage of this method is that it uses adherent cells which decreases variability and has been proven robust with a number of different hPSC lines [17]. A variation of this method which utilized Noggin but not SB43154 was used in our laboratory with hESCs and hiPSCs to produce the cells used for the studies detailed in this thesis.

The differentiation of hNSC to neurons via non-reprogramming methods can be accomplished using growth factors, chemical, physical, and electrical cues to increase the efficiency and speed of the differentiation as well as increasing the functional maturity of the final neurons. Growth factors such as brain-derived neurotrophic factor (BDNF) [18], glial-derived neurotrophic factor [19], and neurotrophin 3 [20] are used to enhance differentiation either by keeping the neural cells alive or directing their differentiation down a specific pathway [21, 22]. Midbrain dopamine neurons, spinal cord motor neurons, ventral forebrain neurons, cortical pyramidal neurons, and spinal cord dorsal interneurons have been successfully derived using these approaches to NSC differentiation [4, 23]. The major issues in this field are slow

differentiation kinetics, low efficiency, low purity of the specified subtype, and low functional maturity of the final cells.

The Importance of Using Human Cells for Neurological Modeling

The differences between using human cells and mouse cells are very important for pluripotent and neural applications due to species variances in the two systems. Although mice are frequently used as an *in vivo* system to model a wide variety of human disorders they have important biological deviations [15, 24, 25]. Differences between mouse and human PSCs *in vitro* include gene expression, required media components, and differentiation response to specific growth factors [15, 26]. These differences require the use of human cells for disease modeling purposes to more accurately represent human specific reactions to pharmacological interventions and investigations of molecular disease bases. The use of rodent derived cell lines has and will continue to be important to the drug discovery process, but it is likely that there will relatively soon be a paradigm shift into using human derived cells in drug discovery and testing applications.

In vivo Mimetic Environment Effects on Cell Behavior

A factor that can have a great effect on the differentiation, viability, proliferation, migration, and other behaviors of *in vitro* cells is the substrate they are plated onto [27-35]. The factors that have been shown to affect cell properties include topography, stiffness, adsorbed growth factors, conductivity, and surface chemistry [13, 31, 36-38]. Specifically in the field of neural tissue engineering it has been shown that even adsorbed protein orientation can significantly influence the differentiation of hNSCs through their effect on cell adhesion to their substrate, highlighting the complexity of cell-matrix interactions [31]. The addition of certain proteins such as Laminin to the substrate can also enhance neurite outgrowth in dorsal root

ganglion cultures [39]. Chemically distinct regions of a silicone surface have been shown to alter the attachment of neuronal cells without changing any other factor [40]. Scaffold conductivity can also influence the behavior of neural cells, even inducing electrical coupling between neural cells and carbon nanotube (CNT) substrates [35].

Cells are traditionally grown on a two dimensional substrate of pretreated plastic. This environment is used because it is simple to use and easy to implement. However, the *in vivo* environment is not faithfully recapitulated using this kind of growth surface. In the human body's tissues cells grow in a three dimensional environment which they can remodel whenever necessary. To better mimic the *in vivo* environment in the *in vitro* setting cells can be grown on a three dimensional scaffold with defined properties. One method to control matrix geometry is electrospinning, which is a process in which a polymer dispersion in an organic solvent is pulled through a syringe by an electric field (**Figure 1-2**). Electrospinning results in the formation of fibrous scaffolds with pore, fiber diameter, and fiber orientation properties which can be altered based on the desire of the manufacturer. Changing any of these parameters, such as fiber diameter, can result in distinct neural subtype differentiation patterns [41]. Fiber orientation has a significant effect on many neural cell behaviors including Schwann cell proliferation, neurite outgrowth, and astrocyte metabolism [33, 42].

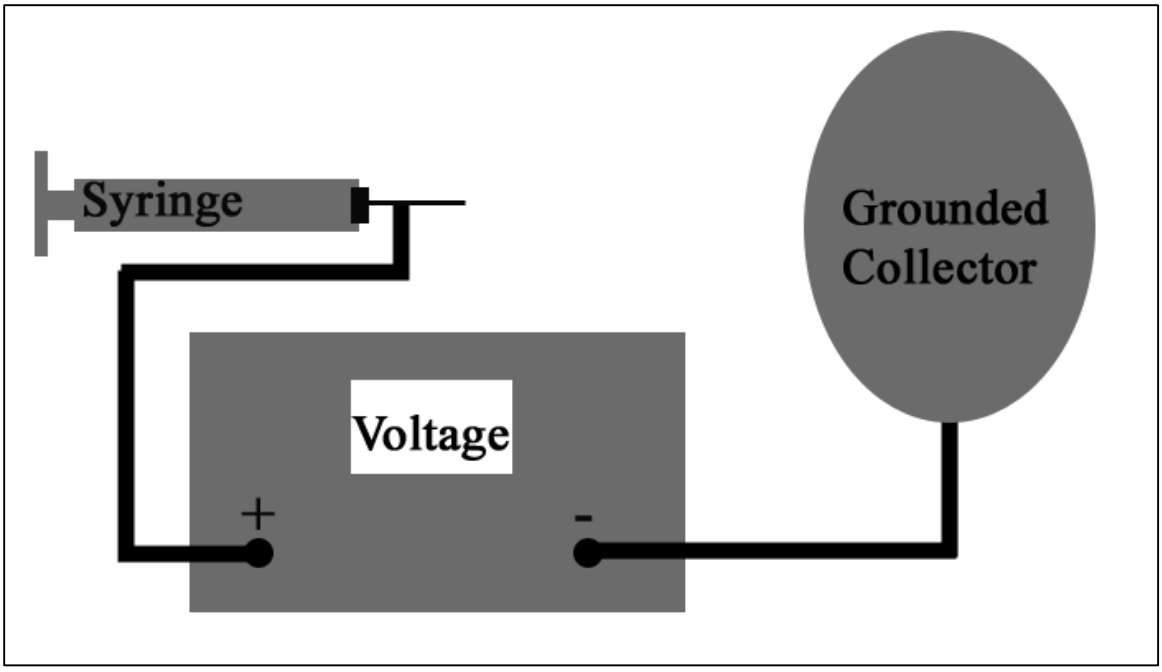

Figure 1-2: Schematic of Electrospinning Apparatus
Electrospinning creates a fibrous scaffold by using an electric field to pull a charged polymeric solution from a syringe needle onto a grounded collector, as shown above. The polymeric solution is extruded at a controlled rate using a syringe pump and a high voltage generator creates a voltage difference typically between 5kV and 20kV between the syringe's needle and the collector, which can be a metal plate or rotating mandrill.

The ability to alter cellular behavior is interesting but not an end unto itself. The important fact about these substrates is that they can be tuned to be *in vivo* mimetic, meaning the surfaces recapitulates act like the environment that a cell would experience while inside the body, the extracellular matrix. With certain stem cells this environmental change induces them to act as if they had been introduced to different parts of the body. For example if a mesenchymal stem cell, a multipotent cell found in adult humans, is placed on a substrate mimicking a bone's surface or that of brain tissue it will differentiate into a cell type similar to the cells normally found in that area of the body [44]. A very interesting study performed by Lai et al investigated the differences in voltage gated calcium channels in primary rat hippocampal neurons on an *in vivo* mimetic three dimensional substrate and a standard two dimensional substrate and compared the results to the results from an organotypic slice of the rat's brain.

The group found that neurons on the two dimensional substrate exhibited a larger calcium influx due to a chemical stimulus than those plated on the three dimensional substrate. The larger stimulus reaction is usually considered superior, but in this case it was shown that the reaction of the three dimensional culture was more similar to the organotypic slice, which is assumed to be essentially an *in vivo* response. The increase in response in the two dimensional culture was therefore an aberrant response, and the three dimensional response was superior because it was more *in vivo* mimetic [45, 46]. The differences in stimulus response were most likely due to the different distribution of voltage gated calcium channels on the membranes of the different surfaces. The altered surface geometry was considered the primary reason for this changed distribution. Therefore the use of *in vivo* mimetic surfaces improves the ability of an *in vitro* culture to accurately model the *in vivo* system.

Carbon Nanotube Surfaces and Properties

CNTs are a very promising material for altering substrate properties due to their inherently high conductivity and their ability to regulate neuronal behavior both structurally and functionally [47]. CNTs have two formats with slightly different properties for our purposes: single-walled carbon nanotubes (SWNT) or multi-walled carbon nanotubes (MWNT). All CNTs are a type of fullerene elongated into a rod [48]. These materials have advantageous properties for multiple fields including high electrical conductivity, high thermal stability and conductivity, high elastic modulus, and small size. CNTs have a high biocompatibility at low concentrations and are ideal candidates for biomedical composites [49]. In particular, CNTs have advantageous properties for devices such as neural electrodes [50].

CNT interfaced with neural cells can promote neuron growth [51-53] and can enhance differentiation of NSCs into neurons [54-57]. This is likely a result of the combination of

topographical cues, enhanced signal transmission from the tight contacts formed between the CNTs and the neuron membranes, and differential production of ECM proteins that modulate synaptic stability [37, 54, 58, 59]. Since CNTs are on the same size scale as neurites their presence acts as an anchor for neural attachment to the substrate and can significantly alter the cellular morphology [60]. Tight contacts formed between CNT and neuron membranes functionally result in a lowered impedance between cell and substrate to boost signal transmission, which causes an increase in the backpropagation of action potentials and the formation of electrical "shortcuts" [59]. Action potential backpropagation has been theorized to increase the neuron's plasticity and ability to interact with its environment [37]. Electrical shortcuts are limited to intracellular shortcuts for the propagation of action potentials; distant neurons cannot connect solely through a CNT substrate. However, neurite outgrowth is hypothesized to be guided by boosted signal transmission towards a direct connection to other neurons [47].

The incorporation of SWNTs into scaffolds that mimic the ECM has proven challenging. Although the addition of CNTs into electrospun fibers is possible and increases conductivity and protein absorption to the scaffold [61], this addition adds an unnecessary degree of complexity to the system [62]. Substrates made from CNTs alone, such as a CNT rope, can provide cues to support neural cell viability and even enhance neurogenesis of rat NSCs [63]. However, this method only allows for coarse control of substrate topography. The use of CNTs during the electrospinning process could be circumvented altogether if the SWNT incorporation or deposition can be designed *post facto*, thus avoiding any bulk modification of the scaffold properties and thereby retaining the SWNT bio-interfacial features. Methods to do so have included spraying CNT onto scaffolds [64] and layer-by-layer deposition [35]. However, these techniques can be tedious to implement, and the growth of CNT onto the scaffolds can leave behind unwanted catalyst particles detrimental to cell viability. An alternative method suggested

in this work employs the vacuum-induced deposition of an aqueous dispersion of SWNT onto a hydrophobic porous substrate. The forced impregnation process affords a facile approach to integrate SWNTs into electrospun polymeric scaffolds without sacrificing the conductive properties of the SWNTs, and importantly retaining high levels of cellular biocompatibility, especially for human neural stem cells that are susceptible to environmental toxins and stress cues.

Electrical Stimulation

The vastly increased conductivity inherent to CNTs allows the use of electrical stimulation through the substrate, possibly increasing the efficacy of the stimulation. Electrical fields are important to neural formation and NSC differentiation *in vivo* and have been recorded in the cerebral cavity in adults as well as during wound healing [65]. Electric fields have been applied to a variety of cell types and elicited a wide range of behaviors with devices such as an agar salt bridge [66]. In a mouse model electric field application for 1 hour at an injury site enhanced dorsal root ganglion regrowth significantly over no treatment and longer time periods, indicating that stimulation should be applied in controlled amounts [67]. *In vitro,* electrical stimulation has been used on mouse NSCs [68] to show enhanced differentiation. Mouse neuroblastoma cells excited through a CNT substrate with electrical currents to see exhibit an electrophysiological response [35]. In a primate model, common marmoset NSCs stimulated by electric fields respond with inward calcium currents [69]. These reports advance the field, but there have been no reports of electrical stimulation with non-cancerous human cells, such as hiPSC derived NSCs, in a scaffold architecture.

Many articles in the literature focus on neurite extension and alignment as the primary endpoint measurement for electrical stimulation. Astrocytes will align to an *in vitro* electric field,

and when neurons are plated onto those astrocytes they will extend their neurites along the astrocytes already in place [51]. Neurite extension is also directly modified by electric field stimulation [70, 71], resulting in increased neurite extension in as little as 10 minutes of stimulation in dorsal root ganglion cultures [53]. Neurite branching however has not been shown to be modified by treatment with electric fields.

The stimulation of neural cells with electrical fields alters many facets of cellular behavior and control including protein manufacture, gene transcription, and signal pathway activation [72]. One of the main activators of signal pathways in developing neurons is BDNF, which is especially involved early and in electrical development [18]. *In vitro* BDNF is used a soluble growth factor to signal NSCs to differentiate to neurons. When electrical fields are used to stimulate the developing cells it has been shown that the two work synergistically to increase neuronal differentiation by sensitizing the cells to the presence of BDNF [18, 66]. In our work BDNF was the main growth factor used to signal neural differentiation of the NSCs to neurons.

In this work, we fabricated SWNT-polymer composite scaffolds using vacuum impregnation within electrospun poly(lactic-co-glycolic acid) (PLGA) membranes, thus rendering the scaffolds electrically conductive. We then modified the composite scaffolds to establish a microniche for a human neural stem cell cultures, where we examined the effect of the composite morphology of the scaffolds on lineage specialization of human neural stem cells toward the neuronal phenotype. Further, we evaluated whether the conductive SWNT component of the scaffolds can promote the neuronal maturation of hiPSC-derived NSCs upon the application of electrical stimulation and found an enhanced effect on the differentiation process. Finally, we concluded that the SWNT composite scaffolds are promising for probing neurogenesis and neural activity, given the high levels of biocompatibility, three-dimensional morphology, extracellular matrix mimetic topography, and tunable differentiation/maturation cues.

References

1. Rouaux, C., S. Bhai, and P. Arlotta, *Programming and reprogramming neuronal subtypes in the central nervous system.* Dev Neurobiol, 2012. **72**(7): p. 1085-98.
2. Takahashi, K., et al., *Induction of pluripotent stem cells from adult human fibroblasts by defined factors.* Cell, 2007. **131**(5): p. 861-72.
3. Bellin, M., et al., *Induced pluripotent stem cells: the new patient?* Nat Rev Mol Cell Biol, 2012. **13**(11): p. 713-26.
4. Cho, M.S., et al., *Highly efficient and large-scale generation of functional dopamine neurons from human embryonic stem cells.* Proc Natl Acad Sci U S A, 2008. **105**(9): p. 3392-7.
5. Matsa, E., et al., *Drug evaluation in cardiomyocytes derived from human induced pluripotent stem cells carrying a long QT syndrome type 2 mutation.* Eur Heart J, 2011. **32**(8): p. 952-62.
6. Yu, J., et al., *Induced pluripotent stem cell lines derived from human somatic cells.* Science, 2007. **318**(5858): p. 1917-20.
7. Yu, J., et al., *Human induced pluripotent stem cells free of vector and transgene sequences.* Science, 2009. **324**(5928): p. 797-801.
8. Pang, Z.P., et al., *Induction of human neuronal cells by defined transcription factors.* Nature, 2011. **476**(7359): p. 220-3.
9. Caiazzo, M., et al., *Direct generation of functional dopaminergic neurons from mouse and human fibroblasts.* Nature, 2011. **476**(7359): p. 224-7.
10. Son, E.Y., et al., *Conversion of mouse and human fibroblasts into functional spinal motor neurons.* Cell Stem Cell, 2011. **9**(3): p. 205-18.
11. Vierbuchen, T., et al., *Direct conversion of fibroblasts to functional neurons by defined factors.* Nature, 2010. **463**(7284): p. 1035-41.
12. Glass, J.D., et al., *Lumbar intraspinal injection of neural stem cells in patients with amyotrophic lateral sclerosis: results of a phase I trial in 12 patients.* Stem Cells, 2012. **30**(6): p. 1144-51.
13. Carlson, A.L., *Engineered Synthetic Microenvironments for Human Pluripotent Stem Cells: Applications for Neuronal Regeneration*, in *Biomedical Engineering*2013, Rutgers University: Piscataway. p. 285.
14. Doetsch, F., *The glial identity of neural stem cells.* Nat Neurosci, 2003. **6**(11): p. 1127-34.
15. Cai, C. and L. Grabel, *Directing the differentiation of embryonic stem cells to neural stem cells.* Dev Dyn, 2007. **236**(12): p. 3255-66.
16. Stern, C.D., *Neural induction: old problem, new findings, yet more questions.* Development, 2005. **132**(9): p. 2007-21.
17. Chambers, S.M., et al., *Highly efficient neural conversion of human ES and iPS cells by dual inhibition of SMAD signaling.* Nat Biotechnol, 2009. **27**(3): p. 275-80.
18. Leng, J., et al., *Brain-derived neurotrophic factor and electrophysiological properties of voltage-gated ion channels during neuronal stem cell development.* Brain Res, 2009. **1272**: p. 14-24.
19. Goto, A., et al., *GDNF and Endothelin 3 Regulate Migration of Enteric Neural Crest-Derived Cells via Protein Kinase A and Rac1.* J Neurosci, 2013. **33**(11): p. 4901-4912.
20. Kalcheim, C., C. Carmeli, and A. Rosenthal, *Neurotrophin 3 is a mitogen for cultured neural crest cells.* Proc Natl Acad Sci U S A, 1992. **89**(5): p. 1661-5.

21. Doi, D., et al., *Prolonged maturation culture favors a reduction in the tumorigenicity and the dopaminergic function of human ESC-derived neural cells in a primate model of Parkinson's disease.* Stem Cells, 2012. **30**(5): p. 935-45.
22. Liu, H. and S.C. Zhang, *Specification of neuronal and glial subtypes from human pluripotent stem cells.* Cell Mol Life Sci, 2011. **68**(24): p. 3995-4008.
23. Gaspard, N. and P. Vanderhaeghen, *From stem cells to neural networks: recent advances and perspectives for neurodevelopmental disorders.* Dev Med Child Neurol, 2011. **53**(1): p. 13-7.
24. Hirst, T.C., et al., *Systematic review and meta-analysis of temozolomide in animal models of glioma: was clinical efficacy predicted?* Br J Cancer, 2013. **108**(1): p. 64-71.
25. Callan, M.A. and D.C. Zarnescu, *Heads-up: new roles for the fragile X mental retardation protein in neural stem and progenitor cells.* Genesis, 2011. **49**(6): p. 424-40.
26. Zhan, M., et al., *Conservation and variation of gene regulation in embryonic stem cells assessed by comparative genomics.* Cell Biochem Biophys, 2005. **43**(3): p. 379-405.
27. Ghasemi-Mobarakeh, L., et al., *Application of conductive polymers, scaffolds and electrical stimulation for nerve tissue engineering.* J Tissue Eng Regen Med, 2011. **5**(4): p. e17-35.
28. Christopherson, G.T., H. Song, and H.Q. Mao, *The influence of fiber diameter of electrospun substrates on neural stem cell differentiation and proliferation.* Biomaterials, 2009. **30**(4): p. 556-564.
29. Xie, J.W., et al., *The differentiation of embryonic stem cells seeded on electrospun nanofibers into neural lineages.* Biomaterials, 2009. **30**(3): p. 354-362.
30. Lu, H.F., et al., *Efficient neuronal differentiation and maturation of human pluripotent stem cells encapsulated in 3D microfibrous scaffolds.* Biomaterials, 2012. **33**(36): p. 9179-9187.
31. Cherry, J.F., et al., *Oriented, Multimeric Biointerfaces of the L1 Cell Adhesion Molecule: An Approach to Enhance Neuronal and Neural Stem Cell Functions on 2-D and 3-D Polymer Substrates.* Biointerphases, 2012. **7**(1-4).
32. Chao, T.I., et al., *Poly(methacrylic acid)-grafted carbon nanotube scaffolds enhance differentiation of hESCs into neuronal cells.* Adv Mater, 2010. **22**(32): p. 3542-7.
33. Subramanian, A., U.M. Krishnan, and S. Sethuraman, *Fabrication of uniaxially aligned 3D electrospun scaffolds for neural regeneration.* Biomed Mater, 2011. **6**(2): p. 025004.
34. Beduer, A., et al., *Elucidation of the role of carbon nanotube patterns on the development of cultured neuronal cells.* Langmuir, 2012. **28**(50): p. 17363-71.
35. Gheith, M.K., et al., *Stimulation of neural cells by lateral layer-by-layer films of single-walled currents in conductive carbon nanotubes.* Advanced Materials, 2006. **18**(22): p. 2975-+.
36. Kraning-Rush, C.M. and C.A. Reinhart-King, *Controlling matrix stiffness and topography for the study of tumor cell migration.* Cell Adh Migr, 2012. **6**(3): p. 274-9.
37. Cellot, G., et al., *Carbon Nanotube Scaffolds Tune Synaptic Strength in Cultured Neural Circuits: Novel Frontiers in Nanomaterial-Tissue Interactions.* Journal of Neuroscience, 2011. **31**(36): p. 12945-12953.
38. Tziampazis, E., J. Kohn, and P.V. Moghe, *PEG-variant biomaterials as selectively adhesive protein templates: model surfaces for controlled cell adhesion and migration.* Biomaterials, 2000. **21**(5): p. 511-20.
39. Swindle-Reilly, K.E., et al., *The impact of laminin on 3D neurite extension in collagen gels.* J Neural Eng, 2012. **9**(4): p. 046007.

40. Sweetman, M.J., et al., *Dual silane surface functionalization for the selective attachment of human neuronal cells to porous silicon.* Langmuir, 2011. **27**(15): p. 9497-503.
41. Christopherson, G.T., H. Song, and H.Q. Mao, *The influence of fiber diameter of electrospun substrates on neural stem cell differentiation and proliferation.* Biomaterials, 2009. **30**(4): p. 556-64.
42. Schaub, N.J. and R.J. Gilbert, *Controlled release of 6-aminonicotinamide from aligned, electrospun fibers alters astrocyte metabolism and dorsal root ganglia neurite outgrowth.* J Neural Eng, 2011. **8**(4): p. 046026.
43. Di Martino, A., et al., *Electrospun scaffolds for bone tissue engineering.* Musculoskelet Surg, 2011. **95**(2): p. 69-80.
44. Engler, A.J., et al., *Matrix elasticity directs stem cell lineage specification.* Cell, 2006. **126**(4): p. 677-89.
45. Lai, Y., K. Cheng, and W. Kisaalita, *Three dimensional neuronal cell cultures more accurately model voltage gated calcium channel functionality in freshly dissected nerve tissue.* PLoS One, 2012. **7**(9): p. e45074.
46. Wu, Z.Z., et al., *Responsiveness of voltage-gated calcium channels in SH-SY5Y human neuroblastoma cells on quasi-three-dimensional micropatterns formed with poly (l-lactic acid).* Int J Nanomedicine, 2013. **8**: p. 93-107.
47. Fabbro, A., et al., *Carbon Nanotubes: Artificial Nanomaterials to Engineer Single Neurons and Neuronal Networks.* Acs Chemical Neuroscience, 2012. **3**(8): p. 611-618.
48. Iijima, S., *Helical Microtubules of Graphitic Carbon.* Nature, 1991. **354**(6348): p. 56-58.
49. Lewitus, D.Y., et al., *Biohybrid Carbon Nanotube/Agarose Fibers for Neural Tissue Engineering.* Advanced Functional Materials, 2011. **21**(14): p. 2624-2632.
50. Kam, N.W., E. Jan, and N.A. Kotov, *Electrical stimulation of neural stem cells mediated by humanized carbon nanotube composite made with extracellular matrix protein.* Nano Lett, 2009. **9**(1): p. 273-8.
51. Alexander, J.K., B. Fuss, and R.J. Colello, *Electric field-induced astrocyte alignment directs neurite outgrowth.* Neuron Glia Biology, 2006. **2**: p. 93-103.
52. Gordon, T., et al., *Brief Electrical Stimulation Accelerates Axon Regeneration in the Peripheral Nervous System and Promotes Sensory Axon Regeneration in the Central Nervous System.* Motor Control, 2009. **13**(4): p. 412-441.
53. Wood, M.D. and R.K. Willits, *Applied electric field enhances DRG neurite growth: influence of stimulation media, surface coating and growth supplements.* Journal of Neural Engineering, 2009. **6**(4): p. 8.
54. Chao, T.I., et al., *Carbon nanotubes promote neuron differentiation from human embryonic stem cells.* Biochemical and Biophysical Research Communications, 2009. **384**(4): p. 426-430.
55. Jan, E. and N.A. Kotov, *Successful differentiation of mouse neural stem cells on layer-by-layer assembled single-walled carbon nanotube composite.* Nano Letters, 2007. **7**(5): p. 1123-1128.
56. Ni, Y.C., et al., *Chemically functionalized water soluble single-walled carbon nanotubes modulate neurite outgrowth.* Journal of Nanoscience and Nanotechnology, 2005. **5**(10): p. 1707-1712.
57. Sridharan, I., T. Kim, and R. Wang, *Adapting collagen/CNT matrix in directing hESC differentiation.* Biochemical and Biophysical Research Communications, 2009. **381**(4): p. 508-512.
58. Lovat, V., et al., *Carbon nanotube substrates boost neuronal electrical signaling.* Nano Letters, 2005. **5**(6): p. 1107-1110.

59. Cellot, G., et al., *Carbon nanotubes might improve neuronal performance by favouring electrical shortcuts.* Nature Nanotechnology, 2009. **4**(2): p. 126-133.
60. Sorkin, R., et al., *Process entanglement as a neuronal anchorage mechanism to rough surfaces.* Nanotechnology, 2009. **20**(1).
61. Liao, H., et al., *Improved cellular response on multiwalled carbon nanotube-incorporated electrospun polyvinyl alcohol/chitosan nanofibrous scaffolds.* Colloids Surf B Biointerfaces, 2011. **84**(2): p. 528-35.
62. Yeo, L.Y. and J.R. Friend, *Electrospinning carbon nanotube polymer composite nanofibers.* Journal of Experimental Nanoscience, 2006. **1**(2): p. 177-209.
63. Huang, Y.-J., et al., *Carbon Nanotube Rope with Electrical Stimulation Promotes the Differentiation and Maturity of Neural Stem Cells.* Small, 2012: p. n/a-n/a.
64. Balani, K., et al., *Plasma-sprayed carbon nanotube reinforced hydroxyapatite coatings and their interaction with human osteoblasts in vitro.* Biomaterials, 2007. **28**(4): p. 618-24.
65. Li, L. and J. Jiang, *Stem cell niches and endogenous electric fields in tissue repair.* Front Med, 2011. **5**(1): p. 40-4.
66. Hronik-Tupaj, M. and D.L. Kaplan, *A review of the responses of two- and three-dimensional engineered tissues to electric fields.* Tissue Eng Part B Rev, 2012. **18**(3): p. 167-80.
67. Geremia, N.M., et al., *Electrical stimulation promotes sensory neuron regeneration and growth-associated gene expression.* Exp Neurol, 2007. **205**(2): p. 347-59.
68. Chang, K.A., et al., *Biphasic electrical currents stimulation promotes both proliferation and differentiation of fetal neural stem cells.* PLoS One, 2011. **6**(4): p. e18738.
69. Shimada, H., et al., *Efficient derivation of multipotent neural stem/progenitor cells from non-human primate embryonic stem cells.* PLoS One, 2012. **7**(11): p. e49469.
70. Cho, Y. and R.B. Borgens, *The effect of an electrically conductive carbon nanotube/collagen composite on neurite outgrowth of PC12 cells.* J Biomed Mater Res A, 2010. **95**(2): p. 510-7.
71. Graves, M.S., et al., *Electrically Mediated Neuronal Guidance with Applied Alternating Current Electric Fields.* Annals of Biomedical Engineering, 2011. **39**(6): p. 1759-1767.
72. Corredor, R.G. and J.L. Goldberg, *Electrical activity enhances neuronal survival and regeneration.* J Neural Eng, 2009. **6**(5): p. 055001.
73. Landers, J., et al., *Carbon Nanotube Composite Scaffolds as Multifunctional Substrates for In Situ Actuation of Differentiation of Human Neural Stem Cells.* Advanced Healthcare Materials, 2013. **_**(_).
74. Sharma, P. and P. Ahuja, *Recent advances in carbon nanotube-based electronics.* Materials Research Bulletin, 2008. **43**(10): p. 2517-2526.
75. Yaglioglu, O., et al., *Wide Range Control of Microstructure and Mechanical Properties of Carbon Nanotube Forests: A Comparison Between Fixed and Floating Catalyst CVD Techniques.* Advanced Functional Materials, 2012. **22**(23): p. 5028-5037.
76. Thostenson, E.T., Z.F. Ren, and T.W. Chou, *Advances in the science and technology of carbon nanotubes and their composites: a review.* Composites Science and Technology, 2001. **61**(13): p. 1899-1912.
77. Luo, X., et al., *Highly stable carbon nanotube doped poly(3,4-ethylenedioxythiophene) for chronic neural stimulation.* Biomaterials, 2011. **32**(24): p. 5551-7.
78. Kleis, J., P. Hyldgaard, and E. Schröder, *Van der Waals interaction of parallel polymers and nanotubes.* Computational Materials Science, 2005. **33**(1–3): p. 192-199.

79. Dresselhaus, M.S., et al., *Raman spectroscopy of carbon nanotubes.* Physics Reports-Review Section of Physics Letters, 2005. **409**(2): p. 47-99.
80. McCullen, S.D., et al., *Characterization of electrospun nanocomposite scaffolds and biocompatibility with adipose-derived human mesenchymal stem cells.* Int J Nanomedicine, 2007. **2**(2): p. 253-63.

Chapter 2 – Composite Substrates of Polymers and Single Walled Carbon Nanotubes: Design and Characterization

Information reported within this chapter also appears in a manuscript submitted to *Advanced Healthcare Materials* in collaboration with Greg Heden and Dr. John Landers in the laboratory of Dr. Alexander Neimark[73]. Greg Heden and Dr. Landers were responsible for development of the vacuum impregnation technique and characterization of the technique via SEM, Raman spectroscopy, and contact angle measurements.

Introduction

Carbon nanotubes (CNTs) were first fabricated and characterized by Ijima using an arc-deposition method reported in 1991[48]. In the last 22 years, CNTs have enabled scientists in the field of electronics to develop new field effect transistors, integrated circuits, and ultra-capacitors with their enhanced and malleable properties compared to standard materials [74, 75]. CNTs are manufactured as single walled nanotubes (SWNT), which consist of a single ring of carbon atoms elongated into a rod, or as multi walled nanotubes (MWNT), which have multiple rings. SWNTs in particular are extremely strong, elastic modulus 10 to 100 times greater than that of steel, have a thermal conductivity greater than diamond, and have 1000 times the current capacity of traditional copper wires [76].

CNT material properties make them intriguing for biological applications. In the neural field CNTs have been proposed as the optimal material for neural electrode manufacture because of their chemical stability, high conductance, and strength, which differentiate them from conductive polymers that can fail *in vivo* during chronic stimulation regimens [77]. Another material with beneficial properties for neural tissue applications are electrospun polymer scaffolds [33]. These scaffolds can alter a neural cell's growth and connectivity substantially by mimicking the extracellular matrix (ECM) [41]. We hypothesize that the addition of SWNT to an electrospun polymer scaffold will have benefits to the formation of neural circuits. However, while multi-walled carbon nanotubes (MWNTs) have been incorporated into the electrospinning process [61], the consistent incorporation of SWNTs into

scaffolds that mimic the ECM has proven relatively challenging [62]. The use of SWNTs during the electrospinning process could be circumvented altogether if the SWNT incorporation or deposition can be designed *post facto*, thus avoiding any bulk modification of the scaffold properties and thereby retaining the SWNT bio-interfacial features. Methods to do so have included spraying CNT onto scaffolds [64] and layer-by-layer deposition [35]. However, these techniques can be tedious to implement, and the growth of CNT onto the scaffolds can leave behind unwanted catalyst particles detrimental to cell viability. The technique presented in this chapter allows the facile integration of SWNT into a prefabricated electrospun scaffold through a process developed in the Neimark laboratory, called vacuum impregnation.

Experimental Design/Methods, Results, and Discussion

Fibrous poly(lactic-co-glycolic acid) (PLGA) scaffolds were fabricated by dissolving 15% weight/volume PLGA (Sigma-Aldrich, 85:15 PLA:PGA) in 1,1,1,3,3,3-Hexafluoro-2-propanol (Sigma-Aldrich, HFIP) with gentle agitation. This solution was electrospun at 3mL/hr via a 23 gauge needle at a potential difference of 18kV and a distance of 18cm onto a grounded flat plate collector. The resulting scaffolds were characterized visually by scanning electron microscopy (SEM), revealing a uniform fibrous architecture (**Figure 2-3**). Their fiber diameter, 1.11µm SD 0.13µm, was determined using ImageJ (NIH).

To incorporate SWNTs into the scaffold, an aqueous dispersion of unfunctionalized SWNT was made containing 0.05%, 0.1%, 0.2%, or 0.4% (weight % by volume) of SWNT (Unidym), bovine serum albumin (BSA, Sigma-Aldrich) and ascorbic acid (Sigma-Aldrich). The dispersion was mixed with a horn tip sonicator (Mixsonix S400) for 10 minutes at a pulsed rate of one second on and one second off at 40 amperes. All chemicals were of reagent grade or higher. A 2 inch by 2 inch PLGA scaffold was placed on a Nalgene 0.2µm pore filter with a 150mL capacity. The scaffold was sealed in place by the upper cup of the filter. A volume of 3 mL of the dispersion was placed onto

the scaffold and pulled through the scaffold by vacuum (**Figure 2-1)**. A visual inspection of the top of the filter used for SWNT impregnation confirmed that the SWNT had infiltrated completely through the scaffold. In addition, a visible black ring on the PLGA scaffold confirmed the presence of SWNT (**Figure 2-2**).

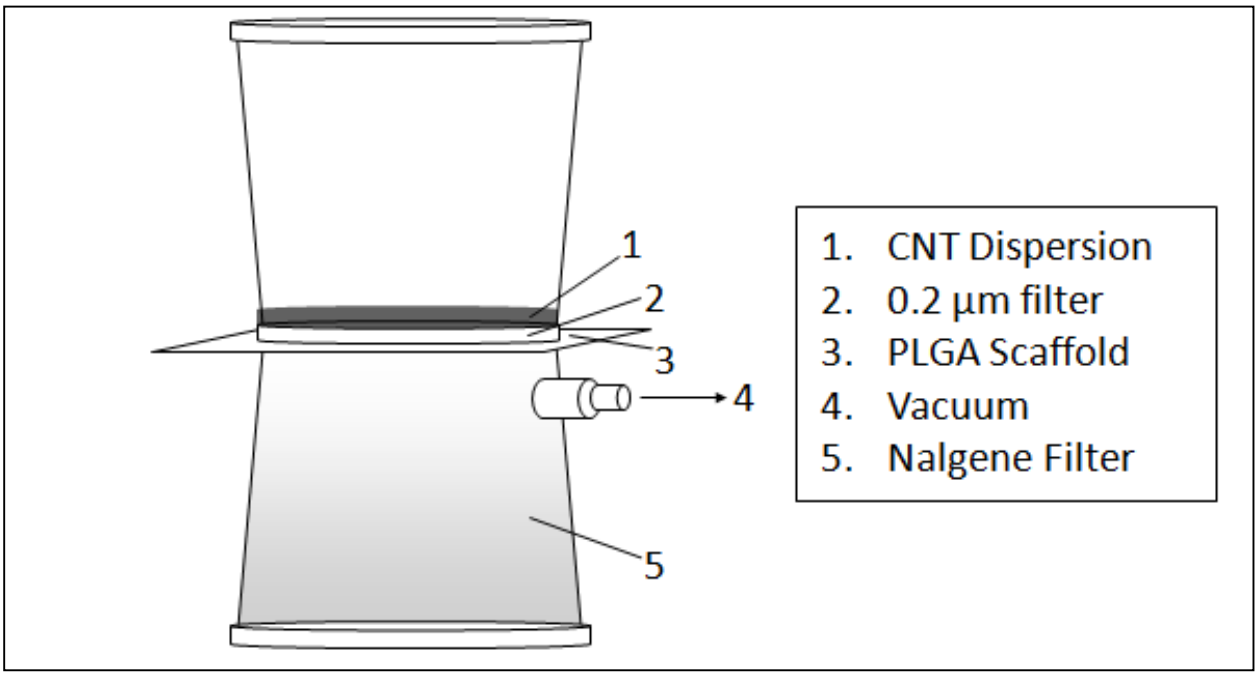

Figure 2-1: Schematic of Vacuum Impregnation System
To perform the vacuum impregnation, a 0.05%-0.4% SWNT dispersion was made using a horn tip sonicator. The top of a Nalgene filtration system held a 2 inch x 2inch PLGA fibrous scaffold in place while 3mL of the SWNT dispersion was spread evenly over the surface. Vacuum was applied through the vacuum port and the SWNT dispersion was forced through the PLGA scaffold to complete the coating process.

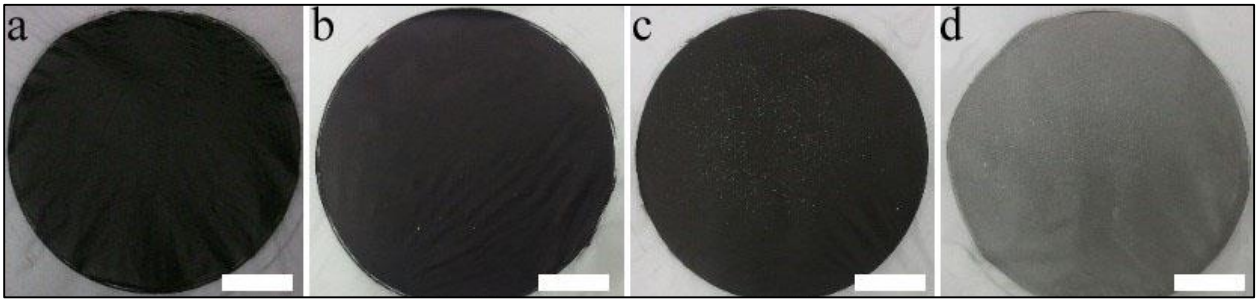

Figure 2-2: Macro View of SWNT-PLGA Composites
The impregnated SWNT left a visible black ring on the macro scale, shown above. a.) 0.4% SWNT-PLGA scaffold. b.) 0.2% SWNT-PLGA scaffold. c.) 0.1% SWNT-PLGA scaffold. d.) 0.05% SWNT-PLGA scaffold. As the amount of SWNTs in the dispersion is reduced, the resultant composite is visibly brighter. Scale bar is 1cm.

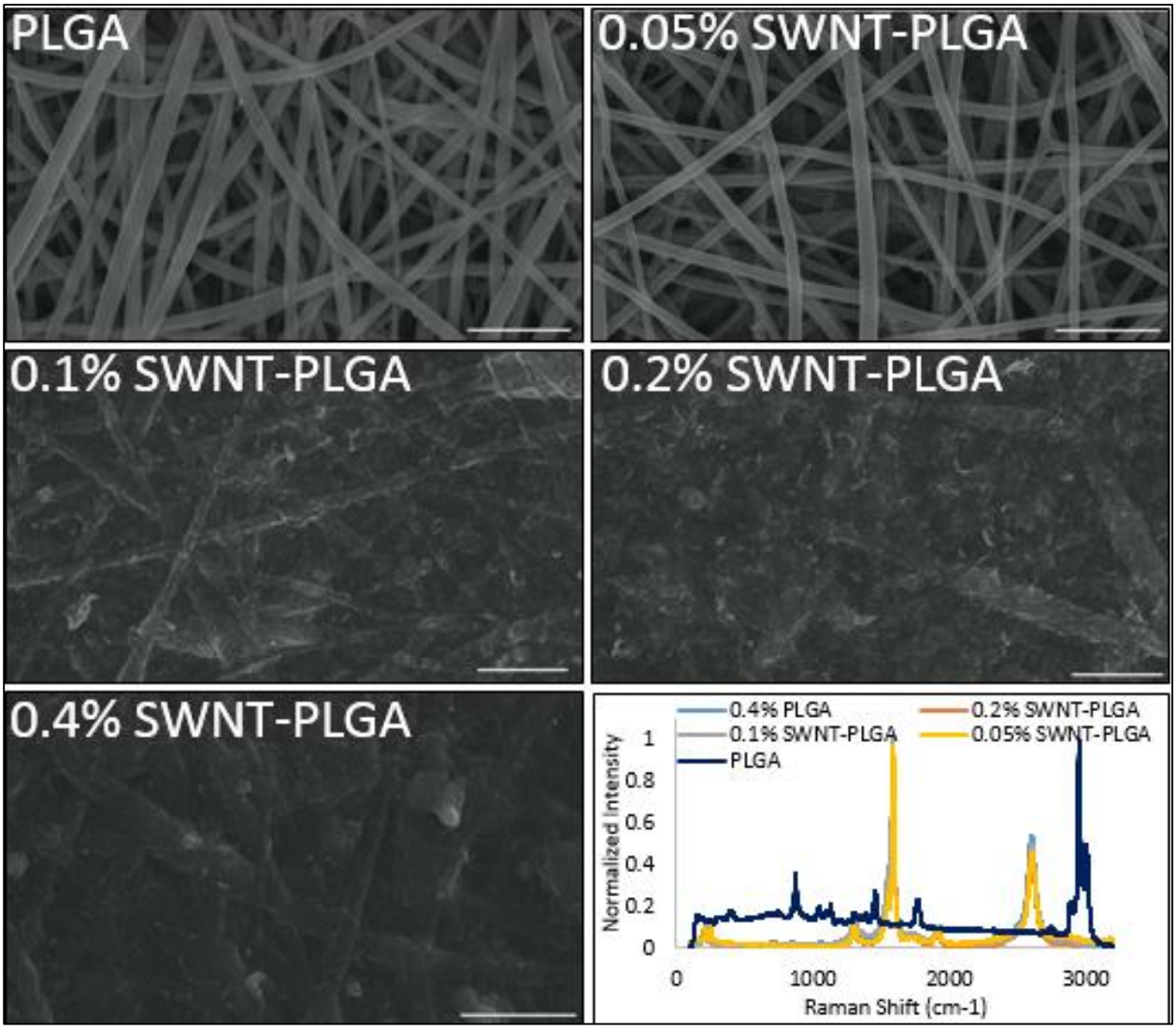

Figure 2-3: SWNT-PLGA Scaffolds: Representative SEM Images and Raman Signatures
Representative SEM images are shown for scaffolds including the original PLGA scaffolds, 0.05%, 0.1%, 0.2%, and 0.4% SWNT-PLGA scaffolds. Above a dispersion concentration of 0.05%, the SWNT filmed over the surface of the PLGA fibrous scaffold, creating a scaffold with a fibrous topology but no porosity. Normalized results from Raman spectroscopy are shown at the bottom right. SWNT characteristic G and G' peaks are located at 1590 and 2700. Scale bars are 10µm.

After allowing the scaffold to dry, SEM images were taken of the scaffold before and after impregnation (**Figure 2-3**). The surface morphology of the fibers within the scaffold changes upon

impregnation with final shape dependent on SWNT dispersion concentration. Scaffolds impregnated with a 0.05% dispersion of SWNT, now referred to as 0.05% SWNT-PLGA, retain their original morphology except for isolated patches in some scaffolds in which aggregated SWNT are seen. For dispersions with SWNT concentrations above 0.05% the SWNT form a film over the fibrous PLGA scaffold. The scaffolds retain a morphology which includes fiber outlines, but the porosity evident in the PLGA and 0.05% SWNT-PLGA scaffolds is no longer present.

The changes in scaffold geometry can be attributed to the presence of aggregated SWNT strongly adsorbed onto the fibers of the scaffold via van der Waals forces [78]. From **Figure 2-3**, a change in contrast can be seen associated with the presence of SWNT in the scaffolds, demonstrating that SWNTs remain adsorbed to the scaffold surface after drying. This could be attributed to the charging associated with the polymeric scaffolds during SEM imaging, a phenomenon consistent with nonconductive samples. The presence of the SWNTs was further confirmed through Raman spectroscopy, which shows characteristic peaks located at 1350, 1590, and 2700 cm^{-1} corresponding to the D, G, and G' peaks inherent to SWNT (**Figure 2-3**) [79]. Each dispersion concentration resulted in a similar Raman signature once impregnated into the PLGA scaffold. The PLGA scaffold without a dispersion added did not contain the characteristic SWNT peaks in its Raman results. The presence of the SWNT are also confirmed via shortwave infrared (SWIR) imaging (**Figure 2-4**) with an excitation wavelength of 980nm, and SWNT response centered at 15nm. The

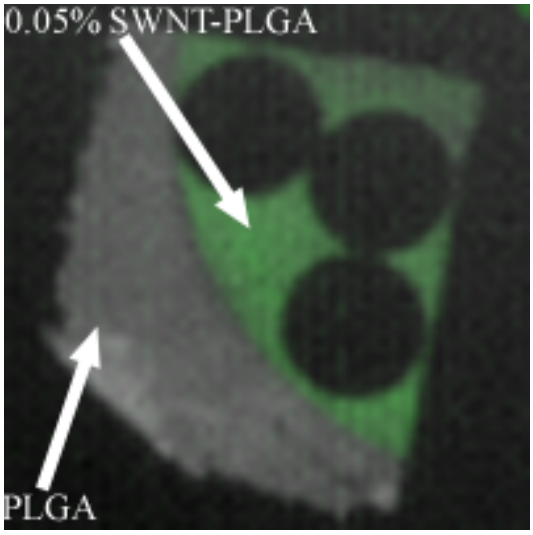

Figure 2-4: SWIR Image of 0.05% SWNT-PLGA SWIR Image of fully excited 0.05% SWNT-PLGA and PLGA scaffold with the green part being the part that had SWNT in it. The excitation wavelength was 980nm and image capture was performed at 1500nm which is typical of SWNT.

entire scaffold shown in **Figure 2-4** was exposed to the excitation wavelength but only the SWNT containing areas showed the green fluorescence.

Water to substrate contact angles were measured to explore the change in hydrophobicity of the surface of the scaffold after wetting. An image of a droplet of distilled water on each scaffold was analyzed in ImageJ (**Figure 2-5**). The PLGA and 0.4% SWNT-PLGA scaffolds were tested and had a contact angle of 117˚ and 80˚, respectively, indicating that the surface chemistry changes markedly with SWNT addition, going from hydrophobic to hydrophilic. This change could increase protein absorption from solution which would affect cell behavior on the substrate. Resistance was also measured on scaffolds containing different concentrations of SWNT. Four random spots on the each scaffold were measured 4cm apart on each side with a digital multimeter (RadioShack) (**Table 1**). Each scaffold made from a dispersion above 0.1% SWNT had a resistance below 5kΩ on the top surface. The 0.05% SWNT-PLGA scaffold was much more conductive than the nonconductive PLGA scaffold, but without the SWNT film formation the resistance is 2 orders of magnitude higher than that of the other SWNT containing scaffolds.

Table 2-1: SWNT Effect on Scaffold Electrical Resistance
Resistance measurements were taken on dry scaffolds with a digital multimeter. n=4

SWNT Concentration	Scaffold Top (kΩ/cm)	Scaffold Bottom (kΩ/cm)
0.40%	1.7	2.3
0.20%	0.4	13.4
0.10%	1.3	4.2
0.05%	169.4	141.0
0.00%	>10,000	-

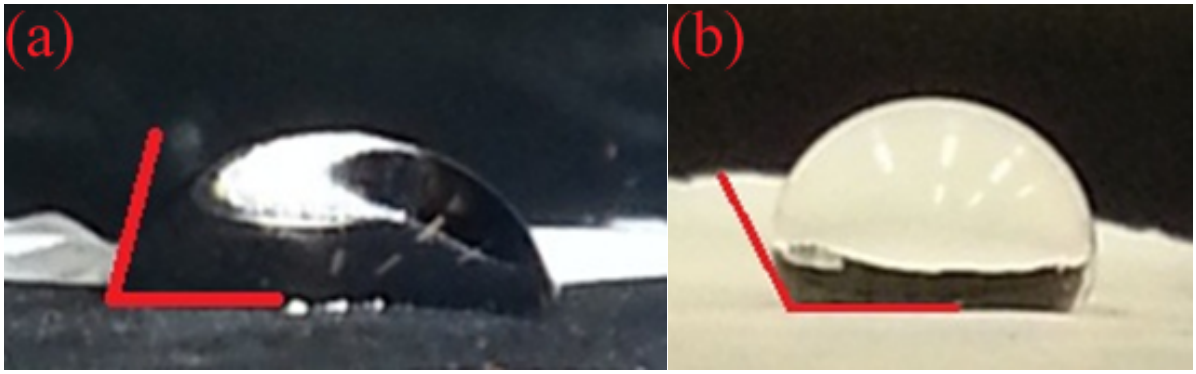

Figure 2-5: Contact Angle Measurements
Contact Angle was measured for the SWNT-PLGA (a) and PLGA (b) scaffolds. The PLGA fiber evidenced a hydrophobic surface with a contact angle of 117˚ while the SWNT-PLGA fibers were more hydrophilic with a contact angle of at 80˚.

To investigate the effect of altering fiber diameter on the impregnation process a second PLGA fiber mat was manufactured with a smaller fiber diameter of 507nm SD 77nm. When the 0.05% SWNT dispersion was driven through the scaffold it had the same effect on the macro and nanoscale features as it had on the larger diameter PLGA scaffold. **Figure 2-6** shows SEM images of the 507nm PLGA scaffold before and after SWNT impregnation. Fiber diameter quantification revealed that in both cases, 1.11µm PLGA and 507nm PLGA, the fiber diameter was not significantly altered by SWNT addition. This result indicates the robustness of this vacuum impregnation technique.

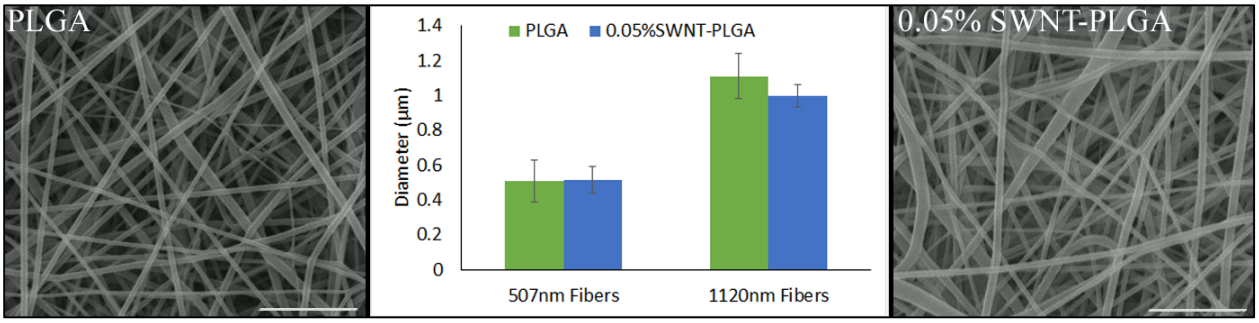

Figure 2-6: 507nm PLGA Fiber Morphology and Wetting
Small diameter, 507nm, PLGA fibers (at left) were manufactured and vacuum impregnation of a 0.05% SWNT dispersion deposited a layer of SWNT onto the fibers (at right). A comparison for fiber diameter changes due to SWNT deposition revealed no significant differences for either the 507nm or 1120nm PLGA fiber sizes. Scale bars are 10µm.

An attempt was also made to produce a composite SWNT-PLGA electrospun scaffold via addition of SWNT to the electrospinning process directly. A final concentration of 0.05% SWNT were added to 15% PLGA in HFIP with bath sonication for 30 minutes used to disperse the SWNT. At a distance of 18cm, voltage of 18kV, and flow rate of 3mL/hr 15% PLGA 0.05% SWNT solution produced fibers with a normal morphology. However, the addition of SWNT did not change the scaffold material properties as expected. At the macroscale there was no darkening of the scaffold which would be expected when black SWNT are added to the normally white PLGA scaffold. SWIR image analysis detected only a faint fluorescence from the co-spun scaffolds compared to the vacuum deposition process (data not shown), and the resistance of the scaffold was higher than the multimeter used could detect, >10MΩ. Transmission electron microscopy (TEM) was employed to search for the SWNT location within the fibers, but the SWNT did not appear to coalesce in any field as reported elsewhere with TEM [8080]. These observations lead us to hypothesize that the bulk of the SWNT did not actually go into the electrospun scaffold. The possibility exists that the bath sonication used to disperse the SWNTs did not function as expected. This co-spinning approach was abandoned in favor of the more promising vacuum impregnation approach for cellular experiments.

Conclusion

In this chapter we manufactured SWNT-PLGA composite scaffolds with a range of geometries and conductance values. These scaffolds were simple to construct and their manufacture has no possibility to leave behind unwanted catalysts because none were involved in the processing. This technique will allow researchers to easily modify existing scaffolds to change parameters such a conductivity and nanoscale roughness. The application of these scaffolds to neural tissue engineering will be discussed in the next chapter.

References

1. Landers, J., et al., *Carbon Nanotube Composite Scaffolds as Multifunctional Substrates for In Situ Actuation of Differentiation of Human Neural Stem Cells.* Advanced Healthcare Materials, 2013. _(_).
2. Iijima, S., *Helical Microtubules of Graphitic Carbon.* Nature, 1991. **354**(6348): p. 56-58.
3. Sharma, P. and P. Ahuja, *Recent advances in carbon nanotube-based electronics.* Materials Research Bulletin, 2008. **43**(10): p. 2517-2526.
4. Yaglioglu, O., et al., *Wide Range Control of Microstructure and Mechanical Properties of Carbon Nanotube Forests: A Comparison Between Fixed and Floating Catalyst CVD Techniques.* Advanced Functional Materials, 2012. **22**(23): p. 5028-5037.
5. Thostenson, E.T., Z.F. Ren, and T.W. Chou, *Advances in the science and technology of carbon nanotubes and their composites: a review.* Composites Science and Technology, 2001. **61**(13): p. 1899-1912.
6. Luo, X., et al., *Highly stable carbon nanotube doped poly(3,4-ethylenedioxythiophene) for chronic neural stimulation.* Biomaterials, 2011. **32**(24): p. 5551-7.
7. Subramanian, A., U.M. Krishnan, and S. Sethuraman, *Fabrication of uniaxially aligned 3D electrospun scaffolds for neural regeneration.* Biomed Mater, 2011. **6**(2): p. 025004.
8. Christopherson, G.T., H. Song, and H.Q. Mao, *The influence of fiber diameter of electrospun substrates on neural stem cell differentiation and proliferation.* Biomaterials, 2009. **30**(4): p. 556-64.
9. Liao, H., et al., *Improved cellular response on multiwalled carbon nanotube-incorporated electrospun polyvinyl alcohol/chitosan nanofibrous scaffolds.* Colloids Surf B Biointerfaces, 2011. **84**(2): p. 528-35.
10. Yeo, L.Y. and J.R. Friend, *Electrospinning carbon nanotube polymer composite nanofibers.* Journal of Experimental Nanoscience, 2006. **1**(2): p. 177-209.
11. Balani, K., et al., *Plasma-sprayed carbon nanotube reinforced hydroxyapatite coatings and their interaction with human osteoblasts in vitro.* Biomaterials, 2007. **28**(4): p. 618-24.
12. Gheith, M.K., et al., *Stimulation of neural cells by lateral layer-by-layer films of single-walled currents in conductive carbon nanotubes.* Advanced Materials, 2006. **18**(22): p. 2975-+.
13. Kleis, J., P. Hyldgaard, and E. Schröder, *Van der Waals interaction of parallel polymers and nanotubes.* Computational Materials Science, 2005. **33**(1–3): p. 192-199.
14. Dresselhaus, M.S., et al., *Raman spectroscopy of carbon nanotubes.* Physics Reports-Review Section of Physics Letters, 2005. **409**(2): p. 47-99.
15. McCullen, S.D., et al., *Characterization of electrospun nanocomposite scaffolds and biocompatibility with adipose-derived human mesenchymal stem cells.* Int J Nanomedicine, 2007. **2**(2): p. 253-63.

Chapter 3 – Human Neural Stem Cell Cultures on SWNT-PLGA Composite Substrates: Studies of Cell Viability and Differentiation

Information reported within this chapter also appears in a manuscript submitted to *Advanced Healthcare Materials*[1].

Introduction

Despite the promise of human neural stem cells (hNSCs) as an emerging cell source for neural tissue engineering, hNSC applications are hindered by the lack of advanced functional biomaterials that can promote cell adhesion, survival, and differentiation while also integrating neuronal stimulatory cues. Traditional two dimensional substrates do not recapitulate the *in vivo* environment in which hNSCs proliferate and differentiate in the human nervous system. Electrospun fibrous scaffolds with controlled fiber architectures provide topographical cues to cells similar to the structure of the extracellular matrix and are capable of enhancing neurite outgrowth and neuronal differentiation of several cell types, including embryonic stem cells and embryonic stem cell-derived hNSCs [2-6]. In addition to stem cells, fibrous scaffolds can support other neural cells, such as Schwann cells, which are essential for neural function *in vivo[7]*.

Substrate conductivity is another major parameter which effects cell behavior[8]. Graphene can improve hNSC differentiation when compared to a standard two dimensional substrate, but graphene is limited in cell culture applications by its necessarily two dimensional geometry [9]. To achieve high levels of conductivity in a fibrous three dimensional scaffold a conductive polymer such as polypyrrole or a material such as carbon nanotubes (CNTs) can be used. On their own conductive polymers have poor mechanical and degradation properties and so are undesirable[10]. However, the increased conductivity imparted by polypyrrole increases enhances mouse neural cell function in a three dimensional substrate [11, 12]. The advantages of carbon nanotubes for neural tissue engineering are superior to those of polypyrrole, graphene, and conductive polymers because of their unique electrical and physical properties. CNTs are

mechanically robust, stronger and more flexible than steel, and are highly electrically conductive due their overlapping π bonds [13]. These features make CNTs more attractive for *in vivo* implantation [14]. CNTs have proven not to be cytotoxic and are compatible with a variety of cell types, assuaging initial concerns about cytotoxicity hindering applications for biological systems, which were likely due to the solubilized nature of CNTs used in these early studies [15-20]. It is not clear if the pathways activated by soluble CNTs, such as the neurotrophin pathway, are effected by non-soluble CNTs [21]. In fact, CNT interaction with mouse and human neuroblastoma lines have suggested that their inclusion into a scaffold might enhance the differentiation of hNSC [16, 22]. In this chapter hNSC were derived from a human induced pluripotent stem cell (hiPSC) line, and the effect of our SWNT-PLGA scaffold on their viability and differentiation to neurons is quantified.

Methods

PLGA Coverslip Fabrication

For a two dimensional control in cellular experiments PLGA thin film coated coverslips were used. To fabricate them, a 1% (w/v) PLGA polymer solution was prepared by dissolving the polymer in HFIP overnight at room temperature. The polymer solution was then spin-coated onto 12 mm glass coverslips. The thin films were dried for at least 24h under vacuum before use.

hiPSC to hNSC Derivation

Induced pluripotent stem cells (HFF1-iPSCs, gift from the Rutgers University Cell and DNA Repository, RUCDR) were grown feeder-free on Matrigel (StemCell Technologies) and fed with the defined media mTeSR (StemCell Technologies). To initiate differentiation to hNSCs the hiPSC's media was switched from 100% mTeSR to 50% mTeSR and 50%neural induction media (NIM) + 500ng/mL Noggin (PeproTech). NIM is comprised of Neurobasal Media (Life Technologies), 1x N2 (Life Technologies), 1x B27 without Vitamin A (Life Technologies), 1x ITS

(Life Technologies), 2mM L-glutamine (Invitrogen), and 0.5% penicillin/streptomycin (Life Technologies). After 5 days the media was switched to 100% NIM+ 500ng/mL Noggin. On Day 13 the cells were passaged using an EZPassage tool (StemPro) onto plates coated with 10ug/mL laminin (Vendor Info) for 2 hours at 37˚C at a 1:5 split ratio and strained using a 40µM cell strainer (Fisher). When cells were 60% confluent the media was switched to Neural Proliferation Media (NPM) which consists of 50% DMEM/F12 + GlutaMAX (Life Technologies) and 50% Neurobasal Media supplemented with 0.5x N2, 0.5x B27 without Vitamin A, 0.5% penicillin/streptomycin, and 20ng/mL bFGF (PeproTech).

Immunocytochemistry Procedure

All cells were fixed by immersing the sample 4% Paraformaldehyde (Fisher), 15 minutes for a sample on a coverslip or 30 minutes for a sample on a scaffold. The sample was then washed 3 times with phosphate buffered saline (PBS). To block and permeabolize the sample it was immersed in a solution PBS based solution of 10% normal goat serum (Fisher), 1% bovine serum albumin (Sigma Aldrich), and 0.1% Triton X (Sigma Aldrich) for one hour a room temperature. All antibody and isotype control solutions were made in 10% normal goat serum and 1% bovine serum albumin and were incubated on the samples for one hour at room temperature. Three washes with PBS, minimum of 15 minutes each, cleared the sample for one hour at room temperature with the secondary, fluorescent antibody. Three washes with PBS followed secondary antibody incubation. DAPI was used to mark the nuclei of each cell and was added at a final concentration of 1µg/mL for 5 minutes to the samples before three PBS washes. Each sample was then mounted onto a glass coverslip using ProLong® Gold Antifade Reagent (Invitrogen) for imaging. All imaging was done on either a Leica SP2 Confocal Microscope or a Nikon Eclipse TE200-S.

Table 1: Antibodies Used in Cell Studies

Antibody targets, dilution factors, and vendors are shown for primary and secondary antibodies.

Antibody Target	Dilution Factor	Vendor	Antibody Target	Dilution Factor	Vendor
MAP2	1:1000	Becton Dickinson	Synaptophysin	1:300	Millipore
Nestin	1:2000	Millipore	TUJ1	1:2000	Covance
NFM	1:500	Invitrogen	mIgG1-488nm	1:500	Invitrogen
Oct4	1:1000	Millipore	mIgG1-594nm	1:500	Invitrogen
Pax6	1:500	Covance	mIgG2a-488nm	1:500	Invitrogen
Sox1	1:300	Neuromics	mIgG2a-594nm	1:500	Invitrogen
SSEA4	1:500	Millipore	rbIgG-488nm	1:500	Invitrogen

Substrate Preparation for Cells and hNSC Seeding Procedure

To prepare the substrates for cells each configuration was sterilized with sequential treatment of 70% ethanol and 100W oxygen plasma for 120 seconds then pretreated with 10µg/mL poly-D-lysine and 20µg/mL Laminin at 37˚C for two hours to promote cell attachment and neurite outgrowth. hNSC were grown to 70-80% confluence and then switched for 2 days to NPM without bFGF after which they were exposed for an additional 2 days to Neural Differentiation Media (NDM) consisting of Neurobasal Media supplemented with 1x B27 without Vitamin A, 1x GlutaMAX (Invitrogen), 0.5% penicillin/streptomycin, and 10ng/ml BDNF (PeproTech) to prime them for differentiation. The cells were harvested using Accutase (Invitrogen) and seeded onto PLGA coverslips, PLGA fibers, or 0.4% SWNT-PLGA scaffolds at 90,000 cells/cm^2 in NDM. One day after cell seeding calcein AM (1µM) and propidium iodide (1µg/mL) were added to the media for 30 minutes at 37˚C. Images of the conditions were taken

on a Leica SP2 confocal microscope and quantified to find the relative amounts of viable and dead cells using ImageJ (NIH).

Calcium Response to Electrical Stimulus

3µM Fluo-4 AM (Invitrogen) was loaded into hNSC in imaging solution which consisted of 140mM NaCl, 5mM KCl, 2mM $CaCl_2$, 2mM $MgCl_2$, 10mM HEPES, and 10mM Glucose, supplemented with 0.2% pluronic F127 (Invitrogen). The chamber consisted of a 2 well LabTek (Thermo Scientific) modified to include a platinum wire on either side of the well, acting as electrodes. To suspend the immersed scaffold for image capture, a coverslip was altered to include 4 plastic pillars, each approximately 1mm high. A second coverslip was placed on top of the pillars, forming a containment space for the sample. Each sample was excited using a 10V pulse train with 10ms pulse width and 100ms pulse spacing. The dye's response was captured at 1Hz on a Leica SP2 Confocal Microscope. Stacks were made from the images in ImageJ and any shifting in the scaffold was corrected using a plugin for normalized correlation coefficient template matching[23]. Each cell in the image was then selected as a region of interest, and the cells' average fluorescence at each frame exported to MATLAB (Example Video in Supplementary Files). A custom MATLAB program detected fluorescence spikes in terms of the change in fluorescence over initial fluorescence (dF/F_0) due to the stimulation with a threshold of a $1dF/F_0$ rise over a 10 second window and calculated the percentage of cells in the frame that showed this activity.

Results & Discussion

hNSC Derivation from hiPSC

The hiPSCs were treated with antibodies against Oct4 and SSEA4 to confirm their pluripotent phenotype (**Figure 3-1**) [24]. The SMAD inhibition method transformed the hiPSCs to obtain a hNSC phenotype[25]. Cells were characterized as hNSC using antibodies for Nestin,

Sox1, and Pax6 (**Figure 3-1**). The positive presence for all three markers indicates an hNSC phenotype.

hNSC Viability on SWNT-PLGA Scaffolds

Since the 0.4% SWNT-PLGA scaffolds were the first developed the majority of the cellular work presented here was done using that scaffold configuration. The 0.4% SWNT-PLGA scaffold also has the advantage of both sides of the scaffold having a stable SWNT film which

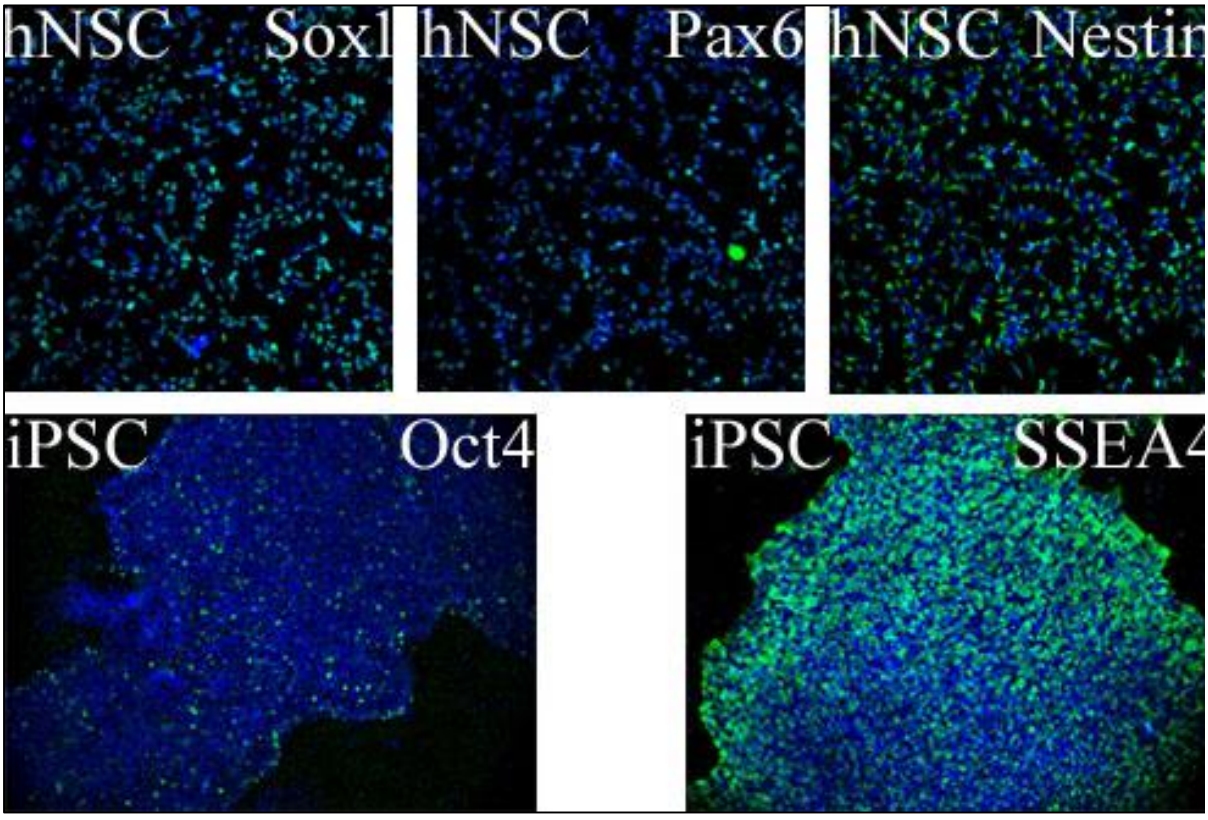

Figure 3-1: **hiPSCs and hNSCs are Phenotypically Normal.**
The top panel shows positive expression for NSC markers Sox1, Pax6, and Nestin as indicated by immunocytochemistry on hNSC. Below, Oct4 and SSEA4, markers of pluripotent stem cells, are shown on the original hiPSC cells, indicating a normal hiPSC phenotype. DAPI (blue) marks the nucleus of each cell and all other markers are green.

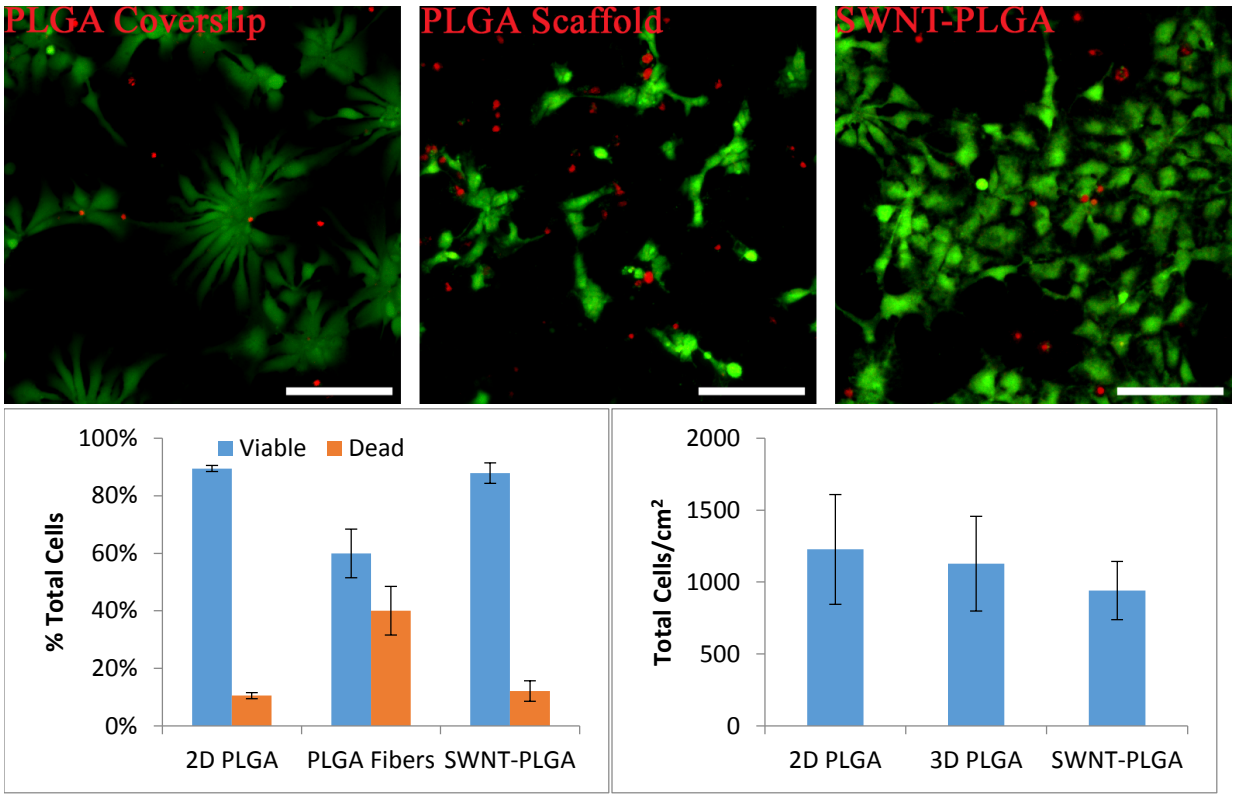

Figure 3-2: hNSC are Viable on 0.4% SWNT-PLGA Substrates.
Cell viability on PLGA coverslips, PLGA scaffolds and SWNT-PLGA scaffolds was measured using calcein AM (viable, green) and propidium iodide (dead, red). Representative images of the three conditions are shown at top with a scale bar of 10µm. The percentage of total cell viability for each condition is shown at the bottom left with total number of cells at bottom right. The PLGA scaffold condition had a significantly lower ($p<0.05$) percentage of total cell viability compared to PLGA coverslip and SWNT-PLGA scaffolds. All conditions had similar numbers of total cells. *Significantly Different from PLGA Scaffold (ANOVA with Bonferroni-Holm Correction) ($p<<.01$)

makes the electrical stimulation discussed in chapter 4 more feasible to implement. hNSC viability was tested on 0.4% SWNT-PLGA scaffolds, PLGA fibrous scaffolds, and PLGA coverslips using calcein AM and propidium iodide to mark viable and dead cells, respectively. The scaffolds were sterilized using oxygen plasma treatment then coated with poly-D-lysine and laminin sequentially. Cell viability on PLGA coverslips and SWNT-PLGA was significantly greater than that on PLGA fibers with no significant differences in the number of cells per condition (**Figure 3-2**). The factor that most likely caused this change is the difference in geometry between the conditions. Between the PLGA coverslip and PLGA fiber conditions the chemical material properties were identical; the major differences were the increased available surface area and

the porosity. These factors make establishing cell to cell contacts more unlikely, which has a negative effect on the viability of these cells. The 0.4% SWNT coating provided a substrate onto which the hNSC were much more viable. The decreased porosity evidenced on the SEM images of the 0.4% SWNT-PLGA versus PLGA fibers (**Figure 2-1**) could have allowed the cells to establish more cell-cell contacts because they were not restricted to extending neurites along fiber tracts. There have also been reports that proteins such as Laminin, which was used on these scaffolds, adsorbs in greater quantity to SWNT coated surfaces[16]; this change is evidenced in our data as an increased hydrophilicity of the SWNT-PLGA versus PLGA fibers.

Immunocytochemistry Quantification of Differentiation

After 1, 7, and 14 days of differentiation within the scaffolds, neuronal differentiation was characterized by evaluating neurofilament M (NFM) and microtubule-associated protein 2 (MAP2) expression, two proteins commonly found in the soma and dendrites of neurons, respectively (**Figure 3-3**). These proteins have been shown to play a critical role in the maintenance of the neuronal architecture, cellular differentiation, and structural and functional plasticity, and are common markers of differentiation from multipotent hNSCs to neuronal cells [26-28]. On day 1 there is little to no expression of either NFM or MAP2 in any condition, indicating that the cells were undifferentiated when seeded on the scaffolds. After 7 days of differentiation, there were 17% NFM+ cells and 17% MAP2+ cells observed in 0.4% SWNT-PLGA scaffolds, compared to 4% NFM+ cells and 9% MAP2+ cells in PLGA scaffolds. While these numbers increased steadily after 14 days of culture to 28% NFM+ cells and 23% MAP2+ cells in 0.4% SWNT-PLGA scaffolds, compared to 10% NFM+ cells and 10% MAP2+ cells in PLGA scaffolds, the clear disparities in fraction of neuronal marker-positive cells between SWNT-containing and SWNT-lacking scaffolds were sustained. Furthermore after 14 days, hNSCs in both scaffold conditions expressed mature neuronal marker synaptophysin (**Figure 3-4**), a

synaptic vesicle protein. qRT-PCR also revealed increased expression of the MAP2 gene at day 14 of differentiation in SWNT-PLGA scaffolds relative to PLGA controls (**Figure 3-2l**).

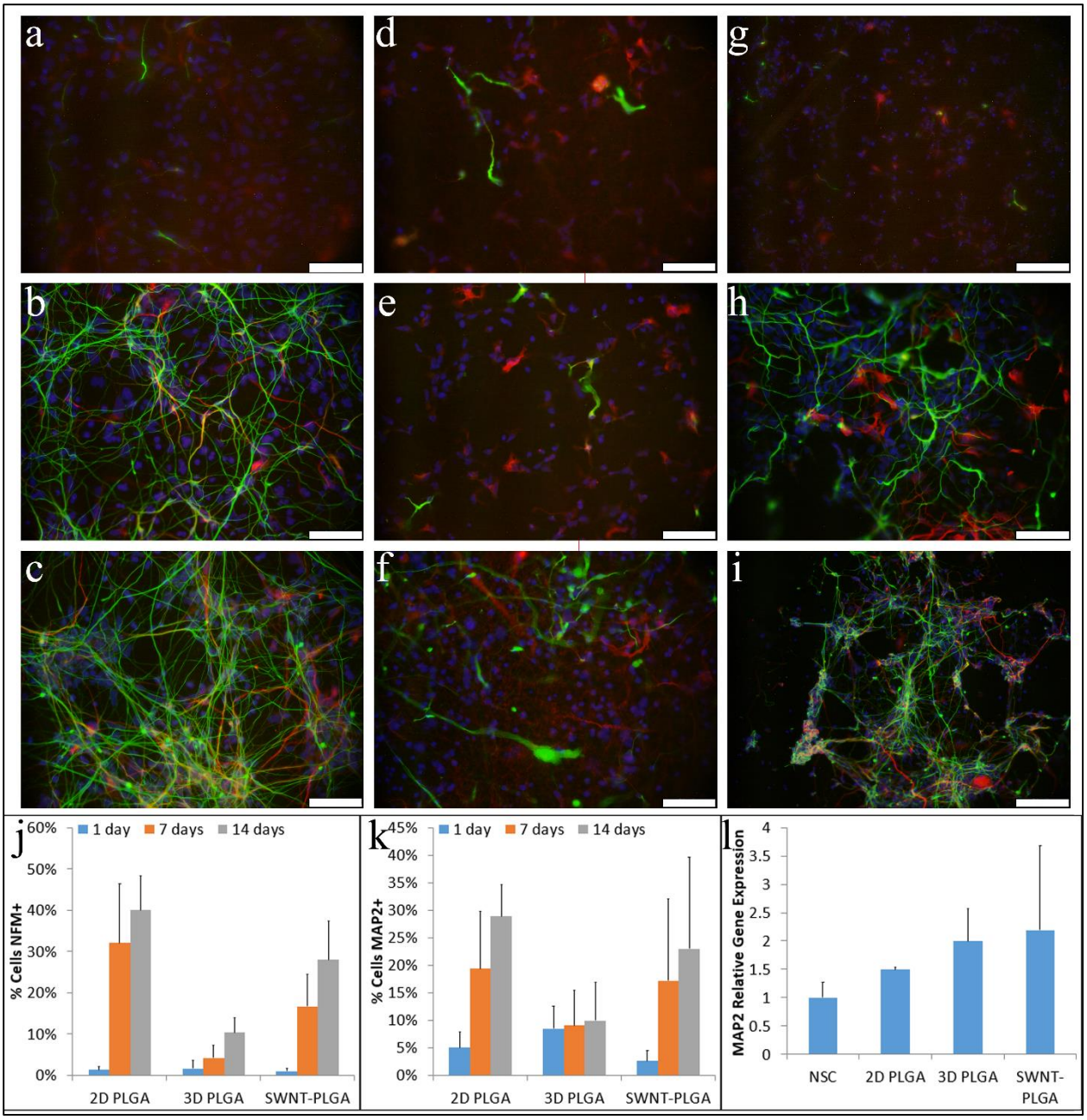

Figure 3-3: SWNT-PGLA scaffolds elicit enhanced neuronal differentiation of hNSCs. hNSCs were cultured on PLGA coverslips (**a-c**), PLGA scaffolds (**d-f**) and 0.4% SWNT-PLGA (**g-i**) scaffolds to determine the effect of SWNT vacuum impregnation on hNSC differentiation. The cells were labeled using antibodies for NFM (green) and MAP2 (red) at 1, 7, and 14 days in the scaffold (**a-i**) The percentage of cells positive for NFM and MAP2 markers are shown (**j & k**). PCR was performed to assay the fold gene expression of MAP2 (**l**). Scale bars are 50µm.

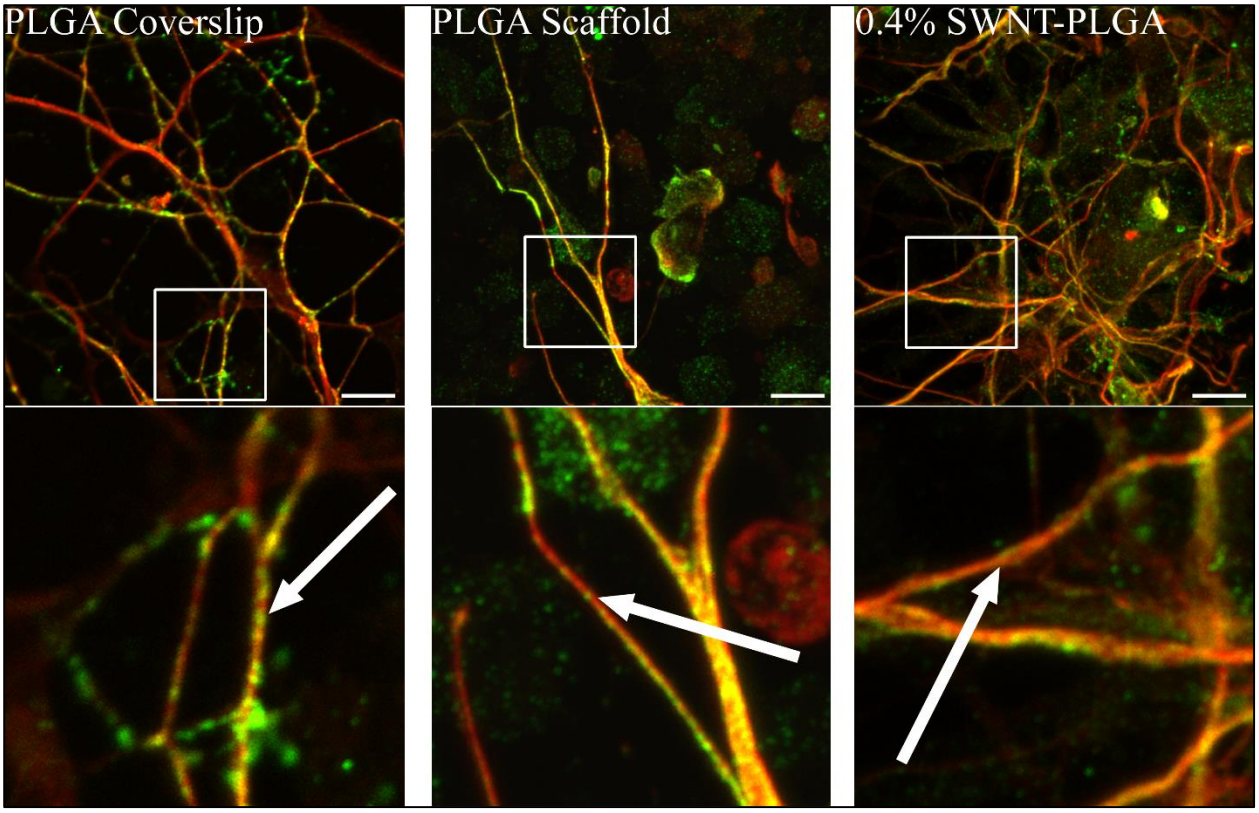

Figure 3-4: Mature Synaptophysin Expression in hNSC.
hNSC grown on PLGA coverslips, PLGA scaffolds, and 0.4% SWNT-PLGA were fixed at day 14 and immunocytochemistry was performed to test for the presence of Synaptophysin (green) and TUJ1 (red). A section of each condition is enlarged with arrows indicating mature, punctate Synaptophysin in the neurites and cell bodies of the cells of both conditions at day 14. Scale bars are 20µm.

Calcium Imaging on SWNT-PLGA Substrates

hNSC electrical activity after 14 days of differentiation was investigated using a calcium indicator dye's fluorescence response to brief electrical stimulation. Electrical stimulation was used to elicit a transient response, not to effect the cells' differentiation. The scaffolds were placed in a special excitation chamber facedown to allow for simultaneous imaging and electrical stimulation and loaded with Fluo-4 AM, a calcium responsive dye (**Figure 3-5a**). For each frame a 60 second baseline was acquired and after 60 seconds a 10V pulse train, 100ms pulse spacing with 10ms pulse width, was applied to the chamber using a Global Specialties 4001 Pulse Generator. The response of the calcium dye was captured at 1Hz using the time lapse feature on a Leica SP2 Confocal Microscope. The results from PLGA coverslips, PLGA scaffolds and 0.4% SWNT-PLGA

scaffolds indicate that the 0.4% SWNT-PLGA scaffolds and PLGA coverslips both cause a significant rise in the percentage of responsive cells compared to the PLGA scaffolds (**Figure 3-5b**). When 1μM tetrodotoxin (TTX) was added to the imaging solution and the cells were stimulated, the rise in calcium levels was decreased so that the percentage of cells firing from the stimulation went to less than 1% of all cells. Since TTX specifically blocks voltage gated sodium channels this is an indication that the increase in calcium fluorescence is most likely due to action potentials. [29] Since one of the major criteria for neuron maturity and functionality is the presence of action potentials this large change in calcium levels is important because it may signal that an action potential is taking place. This measurement is much simpler to get that electrophysiological measurements and has the benefit of being able to give a percentage of firing cells, rather than that single cells are showing mature electrical activity. However, electrophysiology measurements are needed to confirm that the electrical activity is mature to prove that the cells are fully functional.

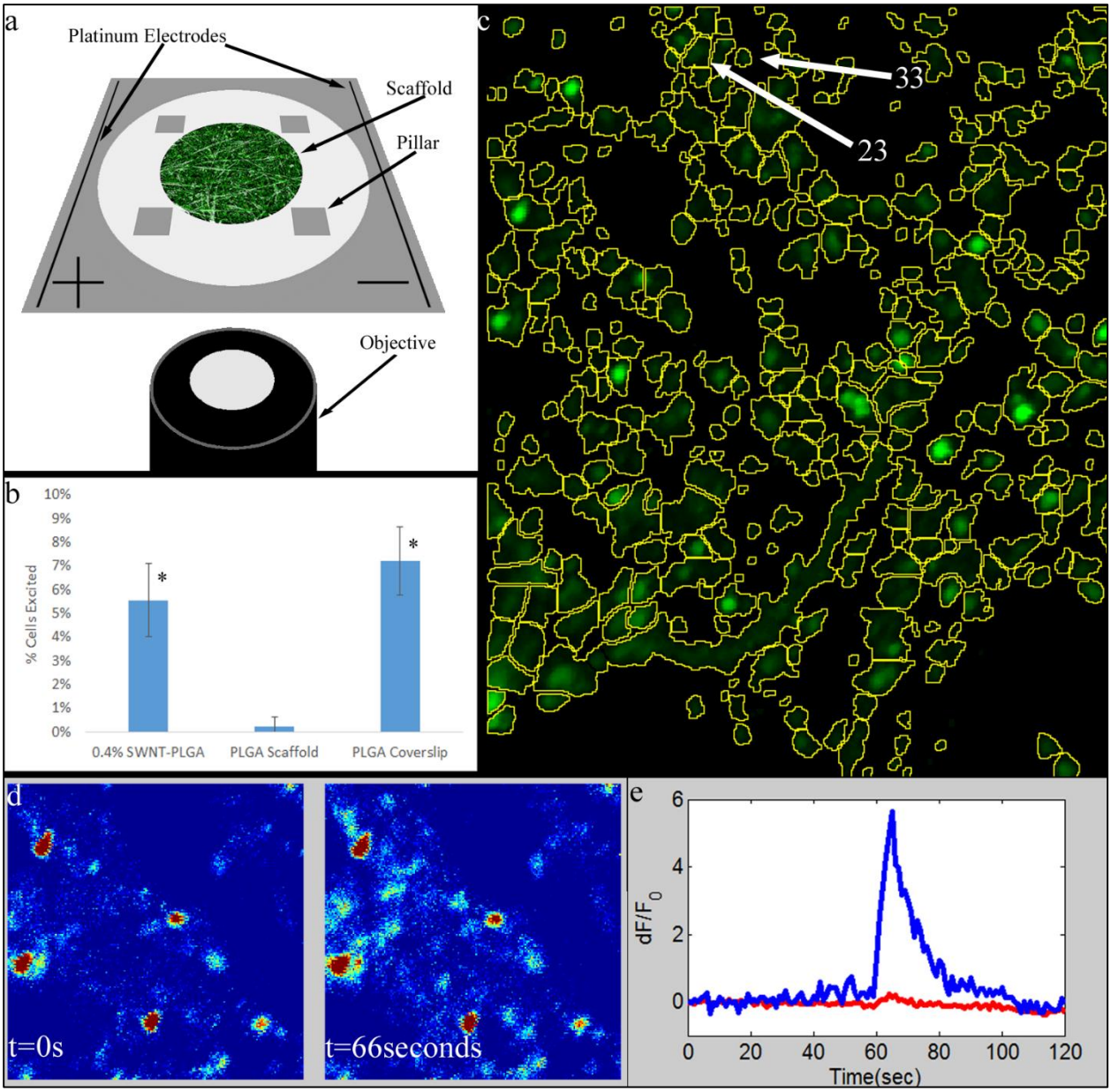

Figure 3-5: Calcium Imaging of hNSC in PLGA and 0.4% SWNT-PLGA Scaffolds

a.) The calcium imaging setup consisted of a downward facing scaffold surrounded by plastic pillars for stabilization and covered with a glass coverslip. b.) Percentage of cells with a response to a 10V pulse train. hNSC in 0.4SWNT-PLGA coverslips had a significantly greater percentage of responsive cells compared to PLGA scaffolds. c.) Example of cell segmentation for calcium dye response quantification. d.) Heat maps of Fluo-4 AM response to a 10V pulse train applied at 60 seconds. Example maps taken at t=0 seconds and t=66 seconds, 6 seconds after the application of a 10V pulse train. e.) Example response of individual cells to a stimulation pulse train applied at 60 seconds. The responsive cell (blue) corresponds to cell number 33 and the nonresponsive cell (red) corresponds to cell number 23. *Significantly Different from PLGA Scaffold (ANOVA with Bonferroni-Holm Correction) ($p<<.01$)

The enhancement of neural differentiation kinetics within 0.4% SWNT-PLGA scaffolds relative to PLGA scaffolds can be attributed to several factors including a change in electrical conductivity, scaffold topography, and scaffold surface chemistry. The increase in conductivity facilitates communication between neuronal cells, by allowing the cells to form “electrical shortcuts”, which facilitate action potential back propagation [17]. This improvement in the neuronal network connectivity has been proposed as the primary mechanism by which CNT increase the frequency of postsynaptic currents [18, 21, 30]. It has also been proposed that these electrical shortcuts could act as crude connections between adjacent cells, boosting signal strength between neurons [18, 21].

In addition to conductivity, scaffold topography has been previously shown to influence various aspects of a cell’s behavior [31] and different cell types will preferentially adhere between two surfaces that, despite having the same surface chemistry, differ in terms of roughness. This has been demonstrated with the use of silicon wafers, where different degrees of roughness can be introduced leading to either adhesive or non-adhesive behavior [32]. For CNT, where the individual form is inherently smooth, their aggregated form displays a significant degree of roughness at the nanoscale [33]. This roughness has been shown to play a critical role in process entanglement which leads to neuronal anchoring onto rough surfaces, which could help to mechanically stabilize the neurons on the surface [34]. Indeed, the change in topography reflected in **Figure 2-1** shows a transformation from fibers with a smooth characteristic to ones with rougher edges. This could partially explain the enhanced differentiation seen in the 0.4% SWNT-PLGA scaffolds.

The addition of the BSA dispersed SWNT changes the surface chemistry of the scaffold, and the presence of BSA could in turn influence further protein adsorption. Chao et al showed that films made from carbon nanotubes grafted with poly(methacrylic acid) (PMAA) provided for

an environment consisting of nanoscale grooves afforded by the CNT, combined with the hydrophobic environment due to the functionalization of PMAA [35]. This in turn led to an increase in a large number of adsorbed proteins, growth factors in particular, essential for the differentiation of hESC to neuronal cells. As noted in the previous chapter the decreased contact angle of the 0.4% SWNT-PLGA substrate compared to the PLGA scaffold could lead to differential protein adsorption to the scaffold surface to influence neural differentiation.

Conclusion

hNSC were successfully derived from hiPSC via growth factor inhibition of the SMAD pathway with Noggin. 0.4% SWNT-PLGA composite scaffolds were found to be highly biocompatible and increased the maturity of hNSC at a faster rate compared to PLGA fibrous scaffolds. hNSC in the 0.4% scaffold exhibited an increased calcium activity in response to electrical stimulation which is of particular interest since electrical activity is an essential part of a neuron's functionality. The composite scaffolds present promising candidates for probing neurogenesis and neural activity, given the high levels of biocompatibility, three-dimensional geometries, extracellular matrix-mimetic topography, and tunable differentiation/maturation cues.

References

1. Landers, J., et al., *Carbon Nanotube Composite Scaffolds as Multifunctional Substrates for In Situ Actuation of Differentiation of Human Neural Stem Cells.* Advanced Healthcare Materials, 2013. _(_).
2. Christopherson, G.T., H. Song, and H.Q. Mao, *The influence of fiber diameter of electrospun substrates on neural stem cell differentiation and proliferation.* Biomaterials, 2009. **30**(4): p. 556-564.
3. Xie, J.W., et al., *The differentiation of embryonic stem cells seeded on electrospun nanofibers into neural lineages.* Biomaterials, 2009. **30**(3): p. 354-362.
4. Lu, H.F., et al., *Efficient neuronal differentiation and maturation of human pluripotent stem cells encapsulated in 3D microfibrous scaffolds.* Biomaterials, 2012. **33**(36): p. 9179-9187.

5. Cherry, J.F., et al., *Oriented, Multimeric Biointerfaces of the L1 Cell Adhesion Molecule: An Approach to Enhance Neuronal and Neural Stem Cell Functions on 2-D and 3-D Polymer Substrates.* Biointerphases, 2012. **7**(1-4).
6. Chao, T.I., et al., *Poly(methacrylic acid)-grafted carbon nanotube scaffolds enhance differentiation of hESCs into neuronal cells.* Adv Mater, 2010. **22**(32): p. 3542-7.
7. Subramanian, A., U.M. Krishnan, and S. Sethuraman, *Fabrication of uniaxially aligned 3D electrospun scaffolds for neural regeneration.* Biomed Mater, 2011. **6**(2): p. 025004.
8. Ghasemi-Mobarakeh, L., et al., *Application of conductive polymers, scaffolds and electrical stimulation for nerve tissue engineering.* J Tissue Eng Regen Med, 2011. **5**(4): p. e17-35.
9. Park, S.Y., et al., *Enhanced Differentiation of Human Neural Stem Cells into Neurons on Graphene.* Advanced Materials, 2011. **23**(36): p. H263-+.
10. Ghasemi-Mobarakeh, L., et al., *Application of conductive polymers, scaffolds and electrical stimulation for nerve tissue engineering.* J Tissue Eng Regen Med, 2011.
11. Xie, J., et al., *Conductive Core-Sheath Nanofibers and Their Potential Application in Neural Tissue Engineering.* Adv Funct Mater, 2009. **19**(14): p. 2312-2318.
12. Bechara, S., L. Wadman, and K.C. Popat, *Electroconductive polymeric nanowire templates facilitates in vitro C17.2 neural stem cell line adhesion, proliferation and differentiation.* Acta Biomater, 2011. **7**(7): p. 2892-901.
13. Dai, H., *Carbon nanotubes: synthesis, integration, and properties.* Acc Chem Res, 2002. **35**(12): p. 1035-44.
14. Fabbro, A., et al., *Carbon Nanotubes: Artificial Nanomaterials to Engineer Single Neurons and Neuronal Networks.* Acs Chemical Neuroscience, 2012. **3**(8): p. 611-618.
15. Liao, H., et al., *Improved cellular response on multiwalled carbon nanotube-incorporated electrospun polyvinyl alcohol/chitosan nanofibrous scaffolds.* Colloids Surf B Biointerfaces, 2011. **84**(2): p. 528-35.
16. Beduer, A., et al., *Elucidation of the role of carbon nanotube patterns on the development of cultured neuronal cells.* Langmuir, 2012. **28**(50): p. 17363-71.
17. Cellot, G., et al., *Carbon nanotubes might improve neuronal performance by favouring electrical shortcuts.* Nature Nanotechnology, 2009. **4**(2): p. 126-133.
18. Cellot, G., et al., *Carbon Nanotube Scaffolds Tune Synaptic Strength in Cultured Neural Circuits: Novel Frontiers in Nanomaterial-Tissue Interactions.* Journal of Neuroscience, 2011. **31**(36): p. 12945-12953.
19. Shao, S., et al., *Osteoblast function on electrically conductive electrospun PLA/MWCNTs nanofibers.* Biomaterials, 2011. **32**(11): p. 2821-33.
20. Dubin, R.A., et al., *Carbon nanotube fibers are compatible with Mammalian cells and neurons.* IEEE Trans Nanobioscience, 2008. **7**(1): p. 11-4.
21. Lovat, V., et al., *Carbon nanotube substrates boost neuronal electrical signaling.* Nano Letters, 2005. **5**(6): p. 1107-1110.
22. Gheith, M.K., et al., *Stimulation of neural cells by lateral layer-by-layer films of single-walled currents in conductive carbon nanotubes.* Advanced Materials, 2006. **18**(22): p. 2975-+.
23. Tseng, Q., et al., *A new micropatterning method of soft substrates reveals that different tumorigenic signals can promote or reduce cell contraction levels.* Lab Chip, 2011. **11**(13): p. 2231-40.
24. Carlson, A.L., *Adaptation of multiple methods for generating human neuronal cells from pluripotent stem cells to 3-dimensional systems*, in *Biomedical Engineering*2013, Rutgers University: Piscataway.

25. Chambers, S.M., et al., *Highly efficient neural conversion of human ES and iPS cells by dual inhibition of SMAD signaling.* Nat Biotechnol, 2009. **27**(3): p. 275-80.
26. Xiong, Y., et al., *Synaptic transmission of neural stem cells seeded in 3-dimensional PLGA scaffolds.* Biomaterials, 2009. **30**(22): p. 3711-22.
27. Zhang, N., et al., *Effects of salvianolic acid B on survival, self-renewal and neuronal differentiation of bone marrow derived neural stem cells.* Eur J Pharmacol, 2012. **697**(1-3): p. 32-9.
28. Yuan, S.H., et al., *Cell-surface marker signatures for the isolation of neural stem cells, glia and neurons derived from human pluripotent stem cells.* PLoS One, 2011. **6**(3): p. e17540.
29. Shimada, H., et al., *Efficient derivation of multipotent neural stem/progenitor cells from non-human primate embryonic stem cells.* PLoS One, 2012. **7**(11): p. e49469.
30. Mazzatenta, A., et al., *Interfacing neurons with carbon nanotubes: Electrical signal transfer and synaptic stimulation in cultured brain circuits.* Journal of Neuroscience, 2007. **27**(26): p. 6931-6936.
31. Fioretta, E.S., et al., *Polymer-based scaffold designs for in situ vascular tissue engineering: controlling recruitment and differentiation behavior of endothelial colony forming cells.* Macromol Biosci, 2012. **12**(5): p. 577-90.
32. Fan, Y.W., et al., *Culture of neural cells on silicon wafers with nano-scale surface topograph.* Journal of Neuroscience Methods, 2002. **120**(1): p. 17-23.
33. Sano, M., et al., *Noncovalent self-assembly of carbon nanotubes for construction of "cages".* Nano Letters, 2002. **2**(5): p. 531-533.
34. Sorkin, R., et al., *Process entanglement as a neuronal anchorage mechanism to rough surfaces.* Nanotechnology, 2009. **20**(1).
35. Chao, T.I., et al., *Carbon nanotubes promote neuron differentiation from human embryonic stem cells.* Biochem Biophys Res Commun, 2009. **384**(4): p. 426-30.

Chapter 4 – Electrical Activity of hNSC on SWNT-PLGA Composite Scaffold

Introduction

The study of bioelectric fields began in 1771 when Luigi Galvani discovered that electricity could force frog leg muscles to contract [1]. In modern times, electrical activity is recognized as an important developmental cue, especially in the nervous system [2, 3]. *In vivo* the presence of electric fields signals for the closure of the neural tube during embryogenesis, neural stem cell (NSC) differentiation and migration in adult cerebral cavities, and direction of the wound healing process [4]. Neural electrical activity on a localized scale, known as action potentials, is the basis for neural signal propagation. To take advantage of electrical fields *in vivo* many groups have developed neural electrodes to directly stimulate brain tissue, but these electrodes are prone to erosion of their metal surfaces and trigger an inflammatory response. The electrode's compliance is also different from that of the brain tissue, causing localized injury and mechanical mismatch [5]. Nevertheless, these electrodes have been successful in the treatment of Parkinson's disease where they can markedly improve patient locomotion [6]. Electrodes manufactured using carbon nanotubes (CNTs) have the potential to solve the degradation and material compliance issues inherent to metal neural electrodes due to CNTs' advantageous material properties [7]. CNT-based substrates are versatile enough to conduct electrical stimulation while being biomcompatible to neural cell types, allowing for the possibility of CNT neuroelectrodes preseeded with NSCs or other cell types.

The use of electric fields *in vitro* to control neural behavior is currently being widely studied. The most obvious effect of electric fields on neurons is the ability to elicit action potentials by depolarizing the cell membrane, which will stimulate existing neural networks. Additionally, electric fields can cause a wide range of effects beyond triggering action potentials. In 1994 it was found that astrocytes exposed to an electric field align their processes perpendicular to the field orientation [8]. Neurons plated on top of those astrocytes match their neurite direction to that

of the astrocytes even in the case of astrocyte fixation [9]. Further, neurites grown from cells in an electric field extend neurites preferentially towards the cathode or anode, depending on the surface on which they are grown, and neurite length is significantly greater in systems with electric field stimulation [10]. This phenomenon parallels work *in vivo* showing that electric fields help regenerate cut neurites in the peripheral nervous system [11]. In an *in vitro* rodent system electrical stimulation was found to promote NSC differentiation in the presence of growth factors, but differentiation without growth factors was more transient [12]. Electric stimulation also regulated proliferation and differentiation in a mouse NSC model [13].

Many of the first studies using electrical stimulation *in vitro* created electric fields using electrodes in a bath solution [2]. More recently scientists have attempted to employ sophisticated electrical stimulation setups using the cell substrate instead of a salt bath solution for signal conduction. Various methods of delivering electrical stimulation to cells in culture include 2-dimensional substrates such as etched indium tin oxide (ITO) glass [14] and conductive polymers in several geometries [10, 15-26]. For example, wires coated with polypyrrole, a conductive polymer, allow the proliferation, survival, and differentiation of mouse NSCs [27]. However, the use of conductive polymers is impeded by their poor mechanical properties and instability. An alternative has emerged involving nanocarbon materials such as CNTs [28, 29] and graphene [30]. Graphene can support the differentiation of fetal hNSCs *in vitro* and can act as an electrode for cellular stimulation [31]. Graphene's necessarily two dimensional nature will constrain its use *in vivo* as will the two dimensionality of similar CNT films, which are difficult to manipulate [29]. For cell culture purposes, the increased flexibility in substrate design obtained through using CNTs over graphene means that CNTs are the more versatile material, allowing the formation of complex scaffolds and materials that better mimic the *in vivo* environment. These scaffold constructs are more easily implantable while retaining their conductivity for electrical

stimulation purposes. Past work in electrical stimulation on CNTs in particular shows promise in encouraging NSC development, but no groups have used a three dimensional CNT substrate in combination with human, phenotypically normal NSCs before this work. For example, applied electrical stimulation increases neurite extension of PC12 cells on a CNT substrate [32]. A CNT-polymer film can excite NG108-15 cells, a type of mouse neuroblastoma cell line, with lateral currents on an indium tin oxide coated glass coverslip, which is evidence of electrical coupling between the CNT surface and the cells [33].

Several beneficial effects of electrical stimulation have been identified to date. One interesting observation is that neurons without electrical activity often undergo apoptosis. This finding has been repeated using a multitude of electrical activity blocking agents [34]. The addition of electrical activity is also neuroprotective in a optic nerve crush model, increasing axon preservation [35]. Electrical activity has been linked to the PI3K/AKT, MAPK, calmodulin-dependent protein kinase, NFκB, and cAMP molecular pathways, all of which can increase neuronal survival [34]. The effect of growth factors without the application of electrical activity is also greatly diminished [36]. In particular, electrical activity appears to have a synergistic relationship with brain-derived neurotrophic factor (BDNF), which is a growth factor important in the electrical development of NSCs. The amount of BDNF needed to trigger an increase in differentiation is decreased with electrical stimulation while BDNF decreases the amount of electrical stimulation needed to see a change in neural cell response to electrical stimulation [2, 34, 37].

In this chapter, we investigate the combined roles of topographical cues of electrospun scaffolds with applied electrical stimulation. For the first time hNSCs derived from hiPSCs are electrically stimulated using a CNT substrate. We hypothesized that our 0.4% SWNT-PLGA scaffolds could deliver an electrical stimulus to cultured hNSCs, and that this electrical stimulation

would enhance neuronal differentiation. We evaluate the effect of this stimulation on hNSC differentiation parameters in terms of neuronal maturation markers (via immunocytochemistry and gene expression readouts), and calcium response to transient electrical stimulation.

Methods

Scaffold Production and Cell Culture

0.4% SWNT-PLGA composite scaffolds are prepared as described in chapter 2 and are fitted with cell culture rings to house the cells and growth media. hNSC are plated as described in chapter 3. Briefly, hiPSC derived hNSC are seeded onto 0.4% SWNT-PLGA scaffolds pretreated with poly(D-lysine) and laminin to promote cell attachment at 90,000 cells/cm^2. The cells are grown in NDM and the media switched every 2-3 days as necessary.

Electrical Stimulation

A circuit board was constructed by Greg Heden in Dr. Neimark's lab at Rutgers University allowing for the application of external electrical stimuli (**Figure 4-1**). Each electrode starts as an ITO covered glass slide. The middle portion is etched with solution of 20% HCl and 5% HNO_3 to create a non-conductive gap, forming two electrodes (**Figure 4-1**) [33]. This conduction method ensures that the applied current travels through the SWNT scaffold and not around a path of least resistance. The ITO glass slide is attached to the metal clips to complete the stimulation circuit. The circuit board has positions for 8 ITO glass slides, and the gaps are bridged with metal wires when not in use. The power source consists of a 1.5 volt watch battery. The ITO glass slides had a resistance of 200 Ω (+/- 50 Ω) whereas the scaffold contained a resistance of 5 kΩ (+/- 2.5 kΩ) on the top and 15 kΩ (+/- 5 kΩ) on the bottom. Electrical stimulation of the cells at 30μA was applied for 10 minutes on the third day of differentiation.

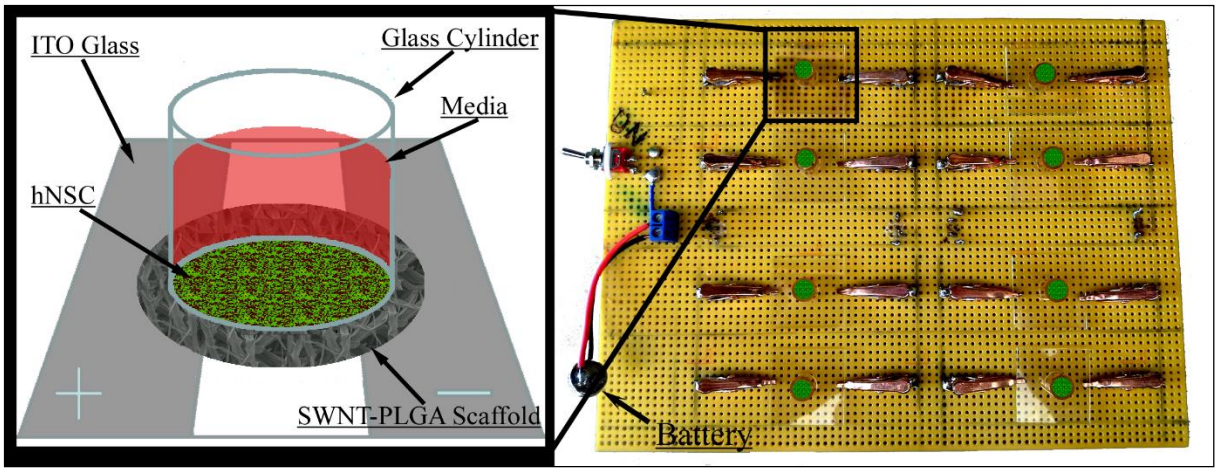

Figure 4-1: Electrical Stimulation Custom Circuit Board
To the left is shown a single scaffold on an etched ITO glass slide. Current flows from the positive electrode through the scaffold to the negative electrode. The scaffold is attached to a glass cylinder to contain the cell media, which allows for scaffold stimulation while on the circuit board and cellular immersion in growth media. To the right is a diagram of a series circuit with the ability to stimulate eight scaffolds simultaneously.

Evaluation of Cellular Differentiation Status

Cell viability was evaluated 24 hours after electrical stimulation using calcein AM and propidium iodide as described in chapter 3. Immunocytochemistry and gene expression studies via RT-PCR were completed for stimulated and unstimulated 0.4% SWNT-PLGA scaffolds at 4 and 11 days after electrical stimulation for a total of 7 and 14 days in the scaffold, respectively, at each time point. Calcium level response to transient electrical stimulation was also performed on day 14 of differentiation in the scaffold for each condition. All procedures were identical to those used in chapter 3.

Results/Discussion

After 3 days of hNSC differentiation in 0.4% SWNT-PLGA scaffolds, a 30μA direct current was applied for 10 minutes through an etched ITO glass slide (**Figure 4-1**). The scaffold-electrode configuration was designed to ensure that current flow through the scaffold to complete the circuit. This mode of electrical stimulation is similar to previously reported methods in terms of duration and electric field strength [10]. Cellular viability analysis using calcein AM and propidium

iodide on the day after stimulation show that the electrical stimulation has a negligible effect on cell viability and the total cell number (**Figure 4-2**). This level of electrical stimulation was not harmful to the hNSC, making it biocompatible. In contrast when a 1.5V battery is connected directly to the scaffold through aluminum foil electrodes the current is an order of magnitude higher and the cellular viability decreases sharply over a 10 minute stimulation window (data not shown). This decreased viability indicates that the hNSCs are being exposed to the stimulation instead of the stimulation bypassing them.

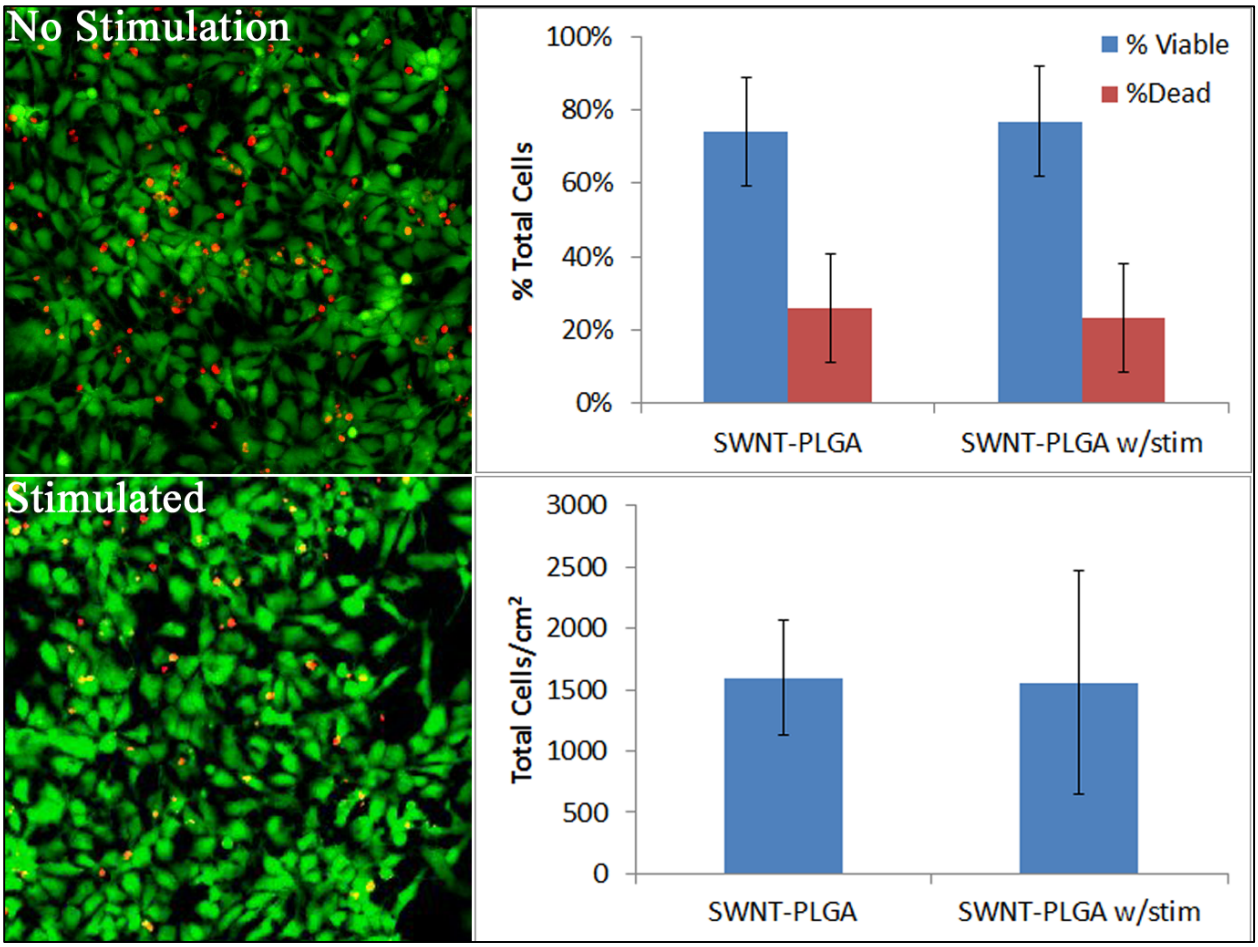

Figure 4-2: Cell Viability is Stable After Electrical Stimulation
One day after electrical stimulation hNSC were labeled with calcein AM (green) and propidium iodide (red) to label viable and dead cells, respectively. Image quantification indicates no significant differences present between stimulated and control scaffolds in the total number of cells per cm^2 or in the percentage of viable cells.

hNSC differentiation was evaluated after 7 and 14 days for 0.4% SWNT-PLGA scaffolds with and without electrical stimulation. After 7 days the percentage of cells positive for NFM and MAP2 is very similar for scaffolds with and without electrical stimulation (**Figure 4-3**). By the 14th day in the 0.4% SWNT-PLGA scaffolds, electrical stimulation increased MAP2 gene expression as measured by qPCR (**Figure 4-4)**, although percentage of MAP2+ cells did not increase (**Figure 4-3**). Previous reports have demonstrated *in vivo* that electrical stimulation can increase MAP2 expression, which can in turn increase dendritic and synaptic plasticity [38]. The number of NFM positive cells increased from 28% to 32% of cells upon electrical stimulation after 14 days in the scaffold. It is interesting to note that the change in MAP2 and NFM expression relative to un-stimulated samples shows a somewhat delayed effect on the expression of these cytoskeletal proteins. While the exact mechanisms are not understood, it is likely that the stimulation activates a pathway far upstream of dendrite formation, possibly increasing dendrite filopodial extension motility or stabilizing existing synaptic connections [39], which results in longer term effects on neuronal differentiation.

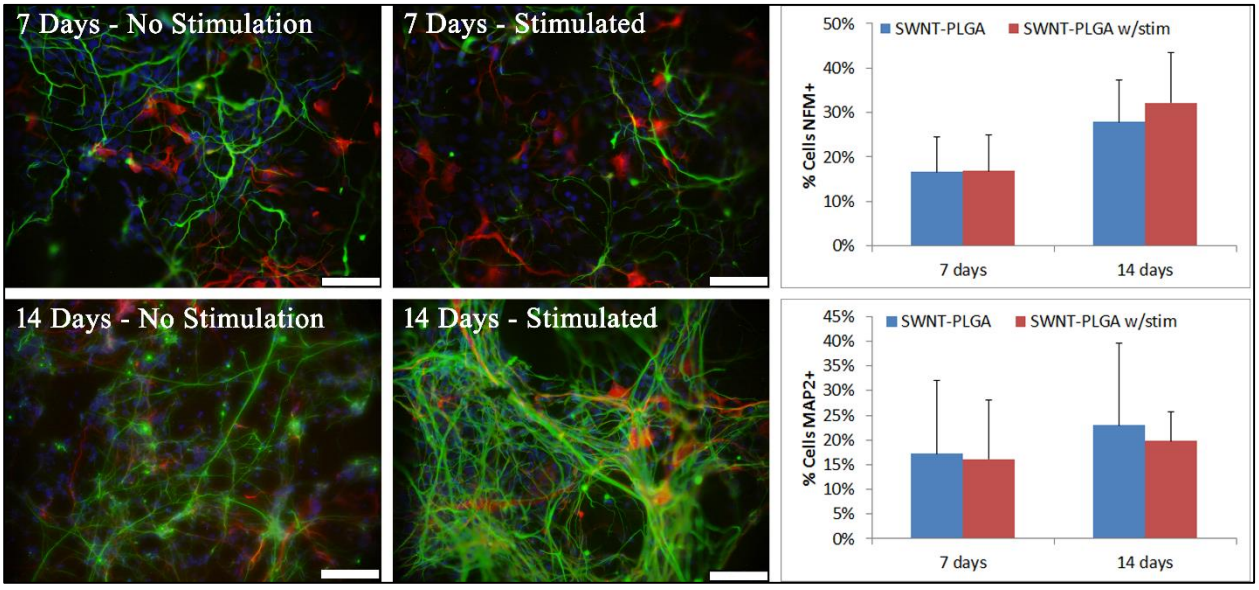

Figure 4-3: Electrical Stimulation Effects on 0.4% SWNT-PLGA Scaffold
Immunocytochemistry evaluated the expression of MAP2 (red) and NFM (green) in hNSCs grown on 0.4% SWNT-PLGA scaffolds for 7 and 14 days. Half of the scaffolds were exposed to 10 minutes

of DC electrical stimulation at 30µA at day 3. The difference in protein expression per cell was analyzed using ImageJ and is shown at right for the percentage of cells expressing NFM (top) and MAP2 (bottom). There is a slight trend upward with stimulation for NFM+ cells and downward for MAP2+ cells. Cell number was determined using DAPI (blue) staining. Scale bars are 50µm.

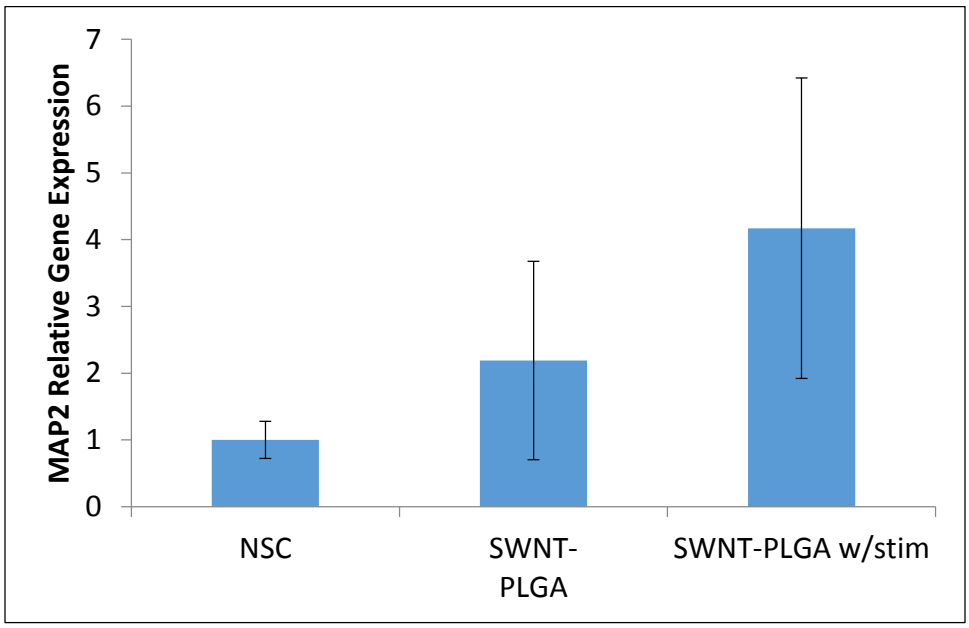

Figure 4-4: MAP2 Gene Expression for Electrically Stimulated hNSC
qRT-PCR identified the MAP2 mRNA expression levels for hNSC after 14 days of differentiation in 0.4% SWNT-PLGA scaffolds with or without electrical stimulation treatment. The electrically stimulated scaffolds tended to have a higher MAP2 gene expression but was not significant when evaluated using a one way ANOVA with Bonferroni-Holm correction.

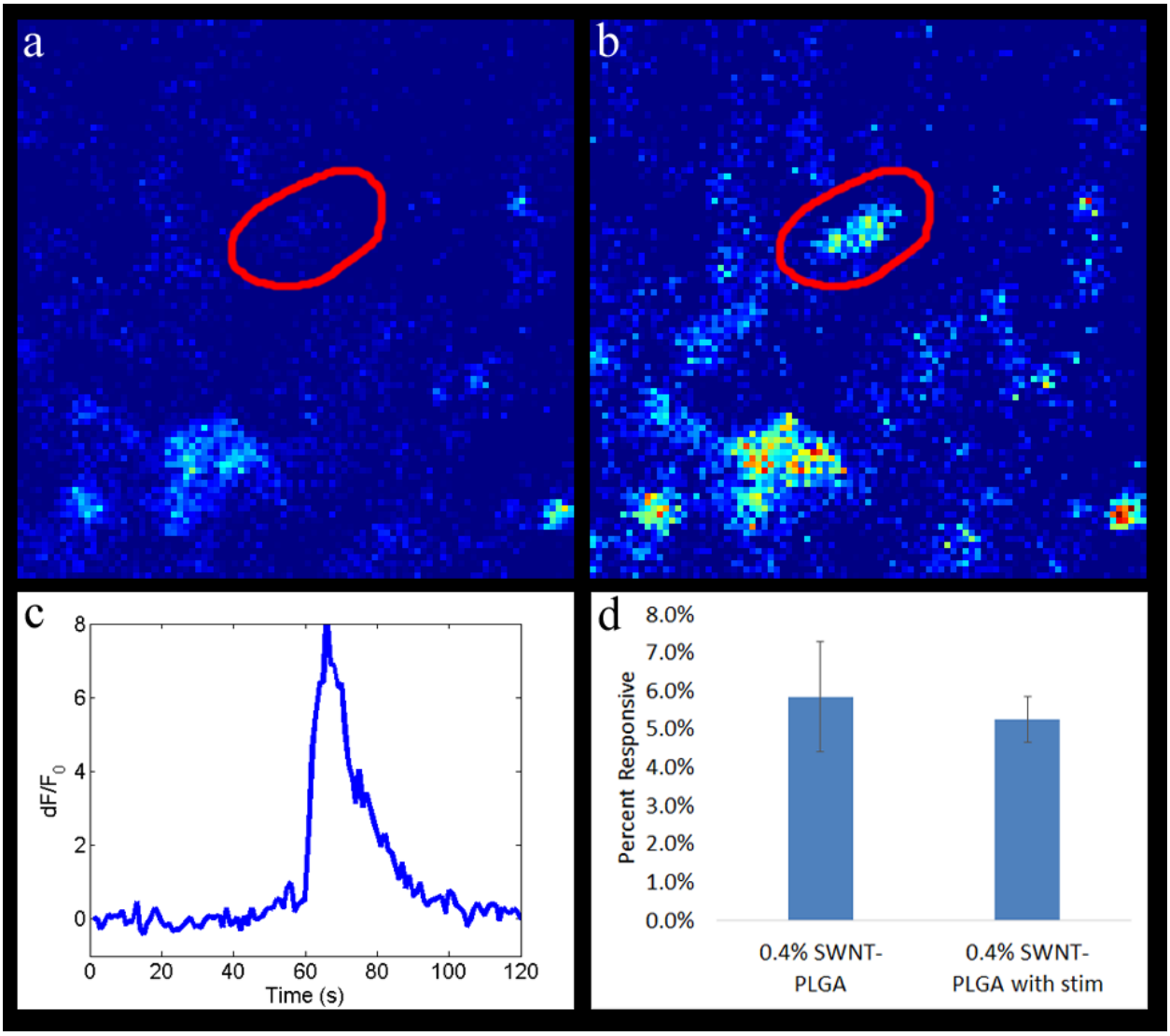

Figure 4-5: hNSC Response to Electrical Stimulation in 0.4% SWNT-PLGA Scaffolds
hNSC grown in 0.4% SWNT-PLGA scaffolds for 14 days were labeled with Fluo-4AM and the calcium levels inside the cells monitored in response to a 10V AC current for 5 seconds. The fluorescence response of a single cell is highlighted before (a) and after (b) electrical stimulation with the accompanying graph of response (c). The stimulation occurred at 60 seconds. There was no change in the overall percentage of cells responding with a calcium influx due to electrical stimulation on the third day in the scaffold, however the stimulated cells' level of response was still significantly higher than the PLGA scaffold condition (d).

The functionality of hNSCs differentiated for 14 days in the 0.4% SWNT-PLGA scaffolds with and without electrical stimulation was assessed by calcium imaging. It was already observed that a greater percentage of cells were functional within SWNT-PLGA scaffolds relative to PLGA

scaffold controls. Similarly, cells were labeled with Fluo-4 AM and time lapse images were acquired to determine the fraction of cells that displayed an increase in intracellular calcium in response to an applied electrical stimulus. A transient 10V, 9Hz AC pulse for 5 seconds was used to stimulate cells. A similar percentage of cells were responsive in stimulated and non-stimulated SWNT scaffolds (**Figure 4-5d**). This demonstrates that while SWNT-PLGA scaffolds improve hNSC functionality, stimulating cells on day 3 of differentiation does not further enhance this effect.

When tabulated, this data is inconclusive in determining the effect of electrical stimulation on hNSC differentiation. While the percent of cells expressing NFM and MAP2 gene expression increase, the percent of cells expressing MAP2 and the percent functional cells do not change. Although in the literature there are examples where 10 minutes of stimulation is enough to change a cell's behavior, those studies investigated the stimulation's effects after 24 hours [40]. In our experiments, it is possible that the method of stimulation used here is having a transient effect or that the effect is too small to be detected. Further optimization of the electrical stimulation parameters could elicit a more robust response in hNSC maturation. The parameters that could be optimized include length of stimulation, type of stimulation (alternating or direct current), current strength, and time course of stimulation application. Identification of optimal methods for stimulating hNSCs within SWNT-PLGA scaffolds would be critical for maximally promoting maturation of these cells to functional neurons. Once the hNSC are maximally differentiated they can be compared to the gold standard of primary mouse neurons, which are currently used for *in vitro* studies of pharmacological agents [41].

Conclusion

In this chapter we investigated delivering electrical stimulation through our 0.4% SWNT-PLGA scaffold using a custom stimulation apparatus. This methodology resulted in no decrease

in cellular viability and increased some markers of hNSC differentiation. *In vitro t*he novel modular design of the setup allows for facile changing of differentiation parameters and can be used to investigate the electrical stimulation response of any cell type plated onto these scaffolds. *In vivo* this composite scaffold's ability to conduct electrical stimulation makes it a candidate for further development as a neuroelectrode.

References

1. Piccolino, M., *Animal electricity and the birth of electrophysiology: the legacy of Luigi Galvani.* Brain Res Bull, 1998. **46**(5): p. 381-407.
2. Hronik-Tupaj, M. and D.L. Kaplan, *A review of the responses of two- and three-dimensional engineered tissues to electric fields.* Tissue Eng Part B Rev, 2012. **18**(3): p. 167-80.
3. McCaig, C.D., et al., *Controlling cell behavior electrically: Current views and future potential.* Physiological Reviews, 2005. **85**(3): p. 943-978.
4. Li, L. and J. Jiang, *Stem cell niches and endogenous electric fields in tissue repair.* Front Med, 2011. **5**(1): p. 40-4.
5. Kam, N.W., E. Jan, and N.A. Kotov, *Electrical stimulation of neural stem cells mediated by humanized carbon nanotube composite made with extracellular matrix protein.* Nano Lett, 2009. **9**(1): p. 273-8.
6. Beuter, A. and J. Modolo, *Delayed and lasting effects of deep brain stimulation on locomotion in Parkinson's disease.* Chaos, 2009. **19**(2): p. 026114.
7. Mazzatenta, A., et al., *Interfacing neurons with carbon nanotubes: Electrical signal transfer and synaptic stimulation in cultured brain circuits.* Journal of Neuroscience, 2007. **27**(26): p. 6931-6936.
8. Borgens, R.B., et al., *Mammalian cortical astrocytes align themselves in a physiological voltage gradient.* Exp Neurol, 1994. **128**(1): p. 41-9.
9. Alexander, J.K., B. Fuss, and R.J. Colello, *Electric field-induced astrocyte alignment directs neurite outgrowth.* Neuron Glia Biology, 2006. **2**: p. 93-103.
10. Schmidt, C.E., et al., *Stimulation of neurite outgrowth using an electrically conducting polymer.* Proceedings of the National Academy of Sciences of the United States of America, 1997. **94**(17): p. 8948-8953.
11. Geremia, N.M., et al., *Electrical stimulation promotes sensory neuron regeneration and growth-associated gene expression.* Exp Neurol, 2007. **205**(2): p. 347-59.
12. Liu, X., et al., *Electrical stimulation promotes nerve cell differentiation on polypyrrole/poly (2-methoxy-5 aniline sulfonic acid) composites.* J Neural Eng, 2009. **6**(6): p. 065002.
13. Chang, K.A., et al., *Biphasic electrical currents stimulation promotes both proliferation and differentiation of fetal neural stem cells.* PLoS One, 2011. **6**(4): p. e18738.
14. Kimura, K., et al., *Gene expression in the electrically stimulated differentiation of PC12 cells.* Journal of Biotechnology, 1998. **63**(1): p. 55-65.
15. Ghasemi-Mobarakeh, L., et al., *Electrical Stimulation of Nerve Cells Using Conductive Nanofibrous Scaffolds for Nerve Tissue Engineering.* Tissue Engineering Part A, 2009. **15**(11): p. 3605-3619.

16. Huang, J.H., et al., *Electrical regulation of Schwann cells using conductive polypyrrole/chitosan polymers.* Journal of Biomedical Materials Research Part A. **93A**(1): p. 164-174.
17. Huang, L.H., et al., *Synthesis of biodegradable and electroactive multiblock polylactide and aniline pentamer copolymer for tissue engineering applications.* Biomacromolecules, 2008. **9**(3): p. 850-858.
18. Jeong, S.I., et al., *Development of electroactive and elastic nanofibers that contain polyaniline and poly(L-lactide-co-epsilon-caprolactone) for the control of cell adhesion.* Macromolecular Bioscience, 2008. **8**(7): p. 627-637.
19. Lee, J.Y., J.W. Lee, and C.E. Schmidt, *Neuroactive conducting scaffolds: nerve growth factor conjugation on active ester-functionalized polypyrrole.* Journal of the Royal Society Interface, 2009. **6**(38): p. 801-810.
20. Rowlands, A.S. and J.J. Cooper-White, *Directing phenotype of vascular smooth muscle cells using electrically stimulated conducting polymer.* Biomaterials, 2008. **29**(34): p. 4510-4520.
21. Shi, G.X., Z. Zhang, and M. Rouabhia, *The regulation of cell functions electrically using biodegradable polypyrrole-polylactide conductors.* Biomaterials, 2008. **29**(28): p. 3792-3798.
22. Sun, S., I. Titushkin, and M. Cho, *Regulation of mesenchymal stem cell adhesion and orientation in 3D collagen scaffold by electrical stimulus.* Bioelectrochemistry, 2006. **69**(2): p. 133-141.
23. Supronowicz, P.R., et al., *Novel current-conducting composite substrates for exposing osteoblasts to alternating current stimulation.* Journal of Biomedical Materials Research, 2002. **59**(3): p. 499-506.
24. Thompson, B.C., et al., *Conducting polymers, dual neurotrophins and pulsed electrical stimulation - Dramatic effects on neurite outgrowth.* Journal of Controlled Release. **141**(2): p. 161-167.
25. Xie, J.W., et al., *Conductive Core-Sheath Nanofibers and Their Potential Application in Neural Tissue Engineering.* Advanced Functional Materials, 2009. **19**(14): p. 2312-2318.
26. Zhang, Z., et al., *Electrically conductive biodegradable polymer composite for nerve regeneration: Electricity-stimulated neurite outgrowth and axon regeneration.* Artificial Organs, 2007. **31**(1): p. 13-22.
27. Bechara, S., L. Wadman, and K.C. Popat, *Electroconductive polymeric nanowire templates facilitates in vitro C17.2 neural stem cell line adhesion, proliferation and differentiation.* Acta Biomater, 2011. **7**(7): p. 2892-901.
28. Chao, T.I., et al., *Carbon nanotubes promote neuron differentiation from human embryonic stem cells.* Biochemical and Biophysical Research Communications, 2009. **384**(4): p. 426-430.
29. Huang, Y.-J., et al., *Carbon Nanotube Rope with Electrical Stimulation Promotes the Differentiation and Maturity of Neural Stem Cells.* Small, 2012: p. n/a-n/a.
30. Park, S.Y., et al., *Enhanced Differentiation of Human Neural Stem Cells into Neurons on Graphene.* Advanced Materials, 2011. **23**(36): p. H263-+.
31. Chao, T.I., et al., *Carbon nanotubes promote neuron differentiation from human embryonic stem cells.* Biochem Biophys Res Commun, 2009. **384**(4): p. 426-30.
32. Cho, Y. and R.B. Borgens, *The effect of an electrically conductive carbon nanotube/collagen composite on neurite outgrowth of PC12 cells.* J Biomed Mater Res A, 2010. **95**(2): p. 510-7.

33. Gheith, M.K., et al., *Stimulation of neural cells by lateral layer-by-layer films of single-walled currents in conductive carbon nanotubes.* Advanced Materials, 2006. **18**(22): p. 2975-+.
34. Corredor, R.G. and J.L. Goldberg, *Electrical activity enhances neuronal survival and regeneration.* J Neural Eng, 2009. **6**(5): p. 055001.
35. Miyake, K., et al., *Neuroprotective effect of transcorneal electrical stimulation on the acute phase of optic nerve injury.* Invest Ophthalmol Vis Sci, 2007. **48**(5): p. 2356-61.
36. Goldberg, J.L., et al., *Retinal ganglion cells do not extend axons by default: promotion by neurotrophic signaling and electrical activity.* Neuron, 2002. **33**(5): p. 689-702.
37. Leng, J., et al., *Brain-derived neurotrophic factor and electrophysiological properties of voltage-gated ion channels during neuronal stem cell development.* Brain Res, 2009. **1272**: p. 14-24.
38. Zhou, Q., et al., *Cortical electrical stimulation alone enhances functional recovery and dendritic structures after focal cerebral ischemia in rats.* Brain Res, 2010. **1311**: p. 148-57.
39. Zhang, L.I. and M.M. Poo, *Electrical activity and development of neural circuits.* Nat Neurosci, 2001. **4 Suppl**: p. 1207-14.
40. Wood, M.D. and R.K. Willits, *Applied electric field enhances DRG neurite growth: influence of stimulation media, surface coating and growth supplements.* Journal of Neural Engineering, 2009. **6**(4): p. 8.
41. Jana, M., et al., *Gemfibrozil, a lipid-lowering drug, increases myelin genes in human oligodendrocytes via peroxisome proliferator-activated receptor-beta.* J Biol Chem, 2012. **287**(41): p. 34134-48.

Chapter 5 – Discussion, Future Directions, and Conclusions

Discussion

In the previous chapters, scaffolds fabricated from synthetic biodegradable polymer, PLGA, and novel carbon nanotube-impregnated polymers (0.4% SWNT-PLGA) were used as substrates for hNSC differentiation and as a platform for electrical stimulation to those cells. The 0.4% SWNT-PLGA substrate is shown to support hNSC growth and to conduct electrical stimulation to those cells. Given the fibrous, extracellular matrix-mimetic geometry of the scaffolds and the intimate nature of CNT-coating of the scaffolds, the system allows for modification of the electrical stimulation parameters, which could prove useful as a tool beyond those offered by other three dimensional cell culture systems. We showed that the addition of a 0.4% SWNT dispersion via vacuum impregnation to the scaffold enhances the differentiation of hNSCs over a 14 day growth period. These scaffold-cell constructs could be utilized as a diagnostic tool to test chemosensory and neurotransmitter-mediated responsiveness for a variety of neurological diseases and disorders if subtype specific neurons are employed.

The mechanisms for the improvements to hNSC differentiation in CNT-scaffolds are not yet elucidated. Some groups have suggested that the reason for improved differentiation in a carbon nanotube containing substrate include increased nanoscale roughness, heightened electrical conductivity, and biologically enhanced scaffold surface chemistry [1-3]. One obvious difference between the two systems is the increased viability of the hNSCs on the 0.4% SWNT-PLGA substrate compared to the PLGA scaffolds. To determine if the topographical changes due to the formation of the SWNT film in the 0.4% SWNT-PLGA scaffold is the cause of the increase in viability compared to PLGA scaffolds, 0.05% SWNT-PLGA scaffolds were used as cellular substrates. The 0.05% SWNT-PLGA scaffolds have the same underlying fibrous architecture as the PLGA scaffolds, which contrasts them vis-a-vis the 0.4% SWNT-PLGA scaffolds. This type of

fibrous architecture has previously been shown to support neurogenesis and has the potential to be more *in vivo* mimetic than a quasi-two dimensional system created by the filming in the 0.4% SWNT-PLGA scaffolds [4-6]. To test the biocompatibility of the 0.05% SWNT-PLGA scaffolds, hNSC were seeded onto the 0.05% SWNT-PLGA scaffolds using the culturing conditions described in chapters 3 & 4. In short, the 0.05% SWNT-PLGA scaffolds and PLGA scaffolds were pretreated with poly(D-lysine) and laminin and then seeded with hNSCs at a density of 90,000 cells/cm^2. Calcein AM and propidium iodide testing after 1 day in the scaffolds confirmed that the viability levels were somewhat low for PLGA scaffolds, as expected, but were significantly higher for cells cultured in 0.05% SWNT-PLGA scaffolds, changing from 64% to 84% with the coating of the smaller concentration of SWNTs (**Figure 5-1**). This finding indicates a positive effect on hNSC viability evidenced by a SWNT coating for fibrous scaffolds, even when the topography is not significantly altered over the microscale as described in chapter 2.

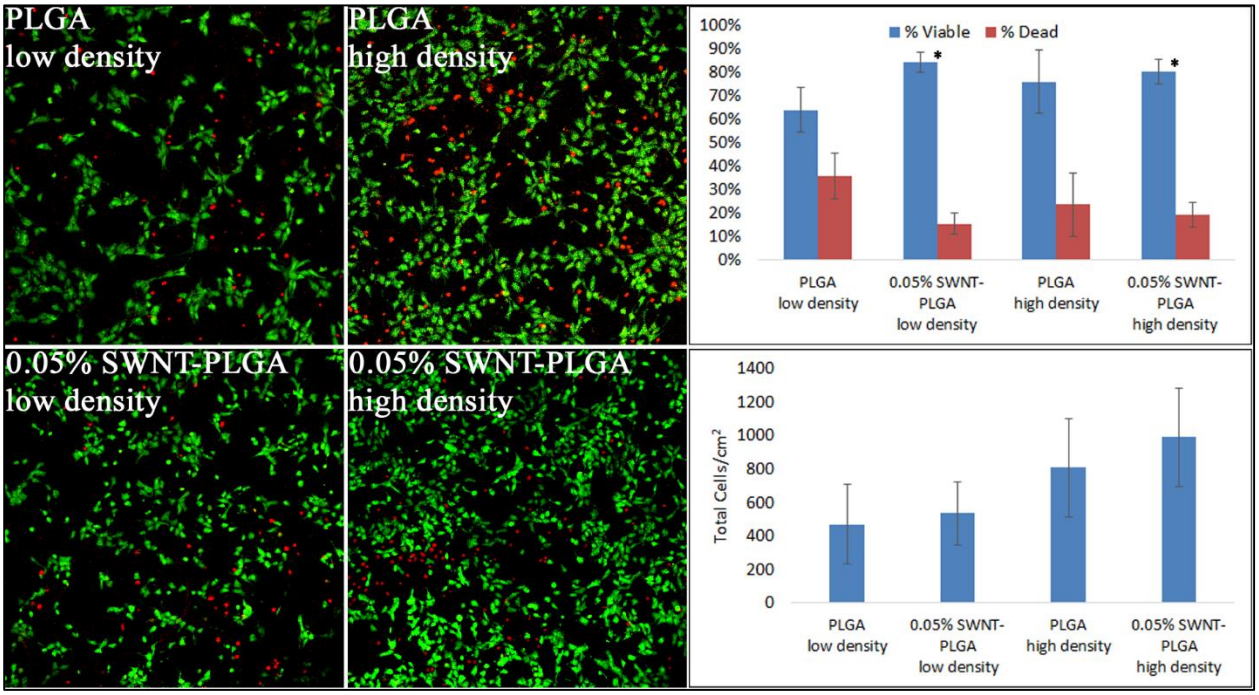

Figure 5-1: hNSC Viability on 0.05% SWNT-PLGA Scaffolds with Increased Seeding Density
hNSC were plated as in chapter 3 onto 0.05% SWNT-PLGA scaffolds and PLGA scaffolds at densities of 90,000 cells/cm^2 and 180,000 cells/cm^2, referred to in the figure panel as low and high density. Cellular viability was evaluated one day after seeding into scaffolds using calcein

AM and propidium iodide. Images were taken using a Leica SP2 Confocal Microscope and quantified using ImageJ.
*Denotes statistical significance evaluated using a one way ANOVA with a Bonferroni-Holm correction.

The decreased viability of hNSCs in the PLGA fibers could potentially trigger a decrease in hNSC differentiation parameters seen in the PLGA scaffolds compared to the 0.4% SWNT-PLGA scaffolds. In an attempt to increase the hNSC viability in the PLGA scaffolds, the seeding density was doubled, under the hypothesis that increased cell to cell contacts would increase viability. After one day of growth in the scaffolds, calcein AM and propidium iodide were used to determine hNSC viability. The result of increasing seeding density in PLGA scaffolds was that hNSC viability in increased from 64% to 76% (**Figure 5-1**). Interestingly, when the hNSC seeding density is doubled for 0.05% SWNT-PLGA scaffolds there was no similar increase in cellular viability, indicating that increased cell to cell contact does not increase cellular viability over the lower range of concentrations of SWNT in SWNT-PLGA scaffolds. For both 0.05% SWNT-PLGA and PLGA scaffolds, however, doubling the number of seeded cells does not double the number of cells observed 1 day later. To test the hypothesis that this increase in viability would enhance the differentiation process, hNSC were grown in PLGA scaffolds when seeded at 90,000 cells/cm^2 and 180,000 cells/cm^2. After 14 days of differentiation the hNSC were labeled with Fluo-4AM and evaluated for calcium influx response to a 10V pulse train electrical stimulus. The percentage of cells responding to the stimulus increases from 0.3% $\pm$ 0.6% to 2.9% ± 3.1% in PLGA scaffolds but is still lower than the 5.9% SD 2.2% observed in the 0.4% SWNT-PLGA scaffolds (**Figure 5-2**). This heightened response could be due to the raised local concentration of hNSCs in the scaffold alone, and since the increase in responsive cells is not significant the decreased viability of hNSC in the PLGA fibers may not be the only factor enhancing the response for the 0.4% SWNT-PLGA scaffold case. We have seen in the past that the

differentiation behavior of these cells is density dependent which is a confounding variable for this experiment. For the future, a logical next step would be to determine what the response of hNSC in the 0.05% SWNT-PLGA scaffolds at both high and low densities would be after 14 days for a better comparison since that geometry is more similar to that of the PLGA scaffold.

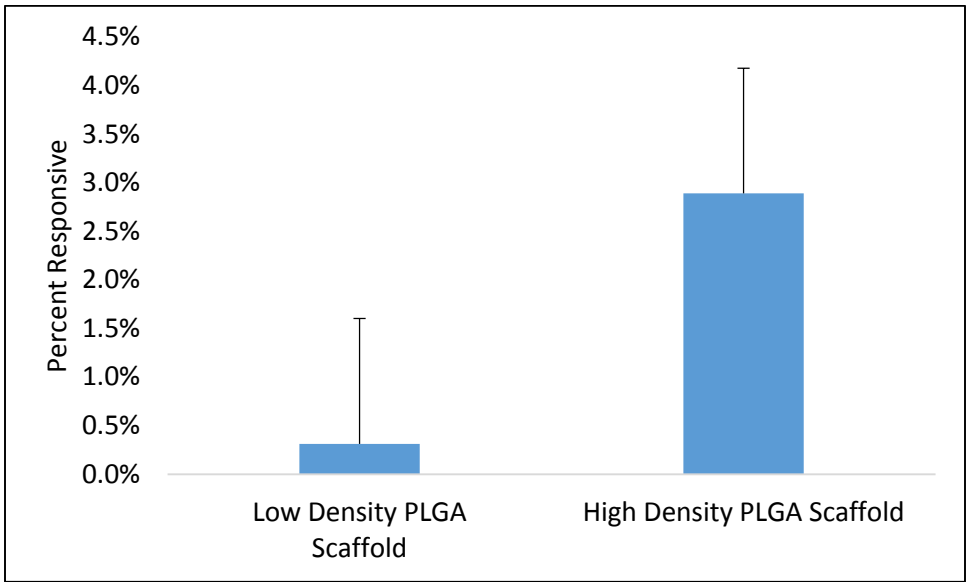

Figure 5-2: Calcium Response of Low and High Density hNSC in PLGA Scaffolds
hNSC were grown in PLGA fibrous scaffolds for 14 days then labeled with Fluo-4AM and exposed to electrical stimulation. A significant increase in fluorescence was defined as 1 dF/F_0 and was recorded at 1Hz. hNSCs in the higher density PLGA scaffold evidenced a slightly higher percentage of responsive cells but the difference was not significant.

Future Directions

In the past *in vitro* human neurological models have been difficult to construct due to the difficulty in harvesting and maintaining primary human neural cells [7]. Our stimulation setup, composed to 0.4% SWNT-PLGA composite scaffold, ITO glass, and circuit board, represents a move forward for the field. By employing a modular design where the stimulation goes through the scaffold and not through the media we allow for a different kind of stimulation which changes the medium through which cells are exposed to electrical stimulation. Additionally, the ability to stimulate multiple scaffolds at once is a large advantage over other

methods where each scaffold must be stimulated individually. The combination of the proposed composite CNT-polymer scaffolds with human neural cells derived from induced pluripotent stem cells could be a useful tool for the study of neurodevelopmental biology or testing of neuronal responsiveness to pharmacological factors. The improved kinetics from hNSCs to neural cells should allow the formation of usably differentiated cells relatively quickly. If region specific neurons are made they could be used to test behaviors such as, for example, the response to dopamine receptor agonists for use in Parkinson's disease. The fact that cells from patients with disease phenotypes could be used is also very significant, allowing for more accurate drug testing scenarios. The *in vivo* mimetic nature of the scaffold should encourage cellular behavior more similar to that of *in vivo* cells, which will translate into more accurate results from *in vitro* testing. This improved accuracy could help to mitigate the significant costs associated with doing animal trials by eliminating more potential drug therapies before they get to the animal trial phase of the process. Additionally, a more predictive *in vitro* assay for neurological disorders could partially alleviate the low correspondence between animal trials and human clinical trials in this system [8, 9]. It is possible that one day these *in vitro* tests are proven to be more accurate than their *in vivo* counterparts since human cells are used here. Likely both methods will always have their place.

From the clinical standpoint, this technology could be used in two distinct ways, the first is as a part of an implantable neural electrode. There have been reports that the properties of CNTs would make an electrode fashioned out of them more resilient to the *in vivo* environment and might cause less of a negative response [10]. In the short term these scaffolds could be implanted in an animal model to evaluate the immune and inflammatory responses evoked by the scaffold. The second major avenue for use is to seed the scaffold with the neural cells with which it is biocompatible before implantation. These cells could then interface with the tissue that the construct is implanted in, lessening immune response or interfacing with the neurons

already there. The first test that would need to be done in that case is to determine if our cells would survive transplantation and the body's response in an animal model.

Conclusions

In this thesis a novel carbon nanotube-polymer composite scaffold manufacturing technique was described and characterized. The scaffolds made using the vacuum impregnation technique allow for the addition of SWNT to existing fibrous scaffolds with different matrix geometries. The SWNT addition is shown to have the effect of enhancing human neural stem cell differentiation. Additionally electrical stimulation passed through the composite scaffold is shown to be non-cytotoxic and may influence the differentiation kinetics of the hNSCs even after very short exposure times. This cell-biomaterial system has the potential to be used for the improved modeling of diseases such as Parkinson's disease as well as operating in the future to improve the accuracy of drug testing platforms.

References

1. Cellot, G., et al., *Carbon Nanotube Scaffolds Tune Synaptic Strength in Cultured Neural Circuits: Novel Frontiers in Nanomaterial-Tissue Interactions.* Journal of Neuroscience, 2011. **31**(36): p. 12945-12953.
2. Fioretta, E.S., et al., *Polymer-based scaffold designs for in situ vascular tissue engineering: controlling recruitment and differentiation behavior of endothelial colony forming cells.* Macromol Biosci, 2012. **12**(5): p. 577-90.
3. Chao, T.I., et al., *Carbon nanotubes promote neuron differentiation from human embryonic stem cells.* Biochem Biophys Res Commun, 2009. **384**(4): p. 426-30.
4. Christopherson, G.T., H. Song, and H.Q. Mao, *The influence of fiber diameter of electrospun substrates on neural stem cell differentiation and proliferation.* Biomaterials, 2009. **30**(4): p. 556-564.
5. Subramanian, A., U.M. Krishnan, and S. Sethuraman, *Fabrication of uniaxially aligned 3D electrospun scaffolds for neural regeneration.* Biomed Mater, 2011. **6**(2): p. 025004.
6. Teo, W.E., W. He, and S. Ramakrishna, *Electrospun scaffold tailored for tissue-specific extracellular matrix.* Biotechnol J, 2006. **1**(9): p. 918-29.
7. Rouaux, C., S. Bhai, and P. Arlotta, *Programming and reprogramming neuronal subtypes in the central nervous system.* Dev Neurobiol, 2012. **72**(7): p. 1085-98.
8. Perel, P., et al., *Comparison of treatment effects between animal experiments and clinical trials: systematic review.* BMJ, 2007. **334**(7586): p. 197.
9. Bullock, M.R., B.G. Lyeth, and J.P. Muizelaar, *Current status of neuroprotection trials for traumatic brain injury: lessons from animal models and clinical studies.* Neurosurgery, 1999. **45**(2): p. 207-17; discussion 217-20.

10. Kam, N.W., E. Jan, and N.A. Kotov, *Electrical stimulation of neural stem cells mediated by humanized carbon nanotube composite made with extracellular matrix protein.* Nano Lett, 2009. **9**(1): p. 273-8.